American Mineralogist, Volume 102, pages 931–947, 2017

Review

A review and update of mantle thermobarometry for primitive arc magmas

Christy B. Till[1,*]

[1]School of Earth and Space Exploration, Arizona State University, Tempe, Arizona 85287, U.S.A.

Abstract

Erupted lavas and tephras remain among the best tools we have to ascertain the mantle processes that give rise to the compositional diversity and spatial distribution of near-primary magmas at volcanic arcs. A compilation of mantle-melt thermobarometry for natural, primitive arc magmas to date reveals published estimates vary between ~1000–1600 °C at ~6–50 kbar. In addition to the variability of mantle melting processes within and between different arcs, this range of conditions is the result of different methodology, such as the nature of reverse fractional crystallization calculations, the choice of thermobarometer, how magmatic H_2O was quantified and its calculated effect on pressure and temperature, and choices about mantle lithology and oxygen fugacity. New and internally consistent reverse fractionation calculations and thermobarometry for a representative subset of the primitive arc samples with adequate published petrography, measured mineral and melt compositions, and constraints on pre-eruptive H_2O content suggest a smaller range of global mantle-melt equilibration conditions (~1075–1450 °C at ~8–19 kbar) than the literature compilation. The new pressure and temperature estimates and major element modeling are consistent with a model whereby several types of primitive arc magmas, specifically hydrous calc-alkaline basalt, primitive andesite and hydrous high-MgO liquid such as boninite, first form at the location of the water-saturated mantle solidus at pressures of ~20–35 kbar and rise into the hot core of the mantle wedge reacting with the mantle en route. Due to their re-equilibration during ascent, these hydrous magmas ultimately record the conditions in the hot, shallow nose of the mantle wedge at the end of their mantle ascent path rather than the conditions at their point of origin as often interpreted. When the mantle residue for this process is lherzolite, calc-alkaline basalt is generated. When the mantle residue is harzburgite to dunite, either high-Mg primitive andesite or high-MgO liquid is generated, depending on the H_2O content. A different type of primitive arc magma, specifically nominally anhydrous arc tholeiite, is generated by near-fractional decompression melting at or near the anhydrous lherzolite solidus in the upwelling back limb of corner flow at ~25–10 kbar and is focused into the same region of the shallow mantle wedge as the hydrous melts. The similarity in the terminus of the mantle ascent paths for both wet and dry primitive arc magmas likely explains their eruption in close spatial and temporal proximity at many arcs. The conditions of last mantle equilibration for primitive arc tholeiites generated by decompression melting also imply that the convecting mantle extends to 10 kbar (~30 km) or less below most arcs. The range of mantle-melt equilibration conditions calculated here agrees well with the range of temperatures predicted for the shallow mantle wedge beneath arcs by geodynamic models, although it suggests some subduction zones may have higher maximum temperatures at shallower depths in the wedge than originally predicted. Primitive hydrous arc magmas also constrain natural variation on the order of 200–250 °C in the maximum temperature in the hot shallow nose of the mantle wedge between arcs. Thus the new primitive magma thermobarometry presented here is useful for understanding melt migration processes and the temperature structure in the uppermost part of the mantle wedge, as well as the origin of different primitive magma types at arcs.

Keywords: Arc, subduction, primitive, barometry, thermometry, mantle, magma, lherzolite, Invited Centennial article, Review article

Introduction

Substantial work has advanced our knowledge of the underlying processes that give rise to volcanic arcs since the advent of plate tectonic theory. This includes an understanding of the first-order processes that produce arc magmas such as models of the volatile flux from the subducting plate into the overlying mantle (e.g., Poli and Schmidt 1995, 2002; Hacker 2008; van Keken et al. 2011) and its effect on mantle melting behavior (Kushiro et al. 1968; Green 1973; Mysen and Boettcher 1975; Kawamoto and

* E-mail: christy.till@asu.edu

0003-004X/17/0005–931$05.00/DOI: http://dx.doi.org/10.2138/am-2017-5783

Holloway 1997; Grove et al. 2006; Till et al. 2012b). Many different types of mantle-derived arc magmas have been observed, including high-Mg andesites, calc-alkaline basalts, high-alumina olivine tholeiites, boninites, and sanukitoids. But questions remain as to what is ultimately responsible for producing each variety of primitive arc magma and why different arcs have different abundances of these magmas. Thermobarometry of the reconstructed primary parental magmas for these primitive liquids provides a powerful means to answer these questions, as well as to determine where in the mantle these primitive liquids are sourced. In addition, thermobarometry of primary arc liquids provides observational constraints on the temperature at a given pressure in the mantle that can be used in conjunction with dynamical models of mantle flow (e.g., Kelemen et al. 2003). Outstanding questions about melt flow in the mantle wedge (e.g., reactive porous flow vs. diapric or channelized flow: Navon and Stolper 1987; Grove et al. 2002) can also for example be addressed through the study of primitive magmas and the pressures and temperatures they record.

The opportunity to answer these questions on a global scale requires a compilation of existing thermobarometry of primitive arc magmas. However, the methodology and assumptions vary between past studies. For example, the process of determining a primitive magma's liquid line of descent in order that the primary liquid composition can be estimated and used with thermobarometers remains somewhat of an art form and thus the methodology and assumptions vary between past studies (e.g., Leeman et al. 2005; Lee et al. 2009; Till et al. 2012a; Kimura et al. 2014). Similarly, the different thermobarometers used in past studies incorporate different assumptions about the mantle residue composition (e.g., harzburgite: Mitchell and Grove 2015 vs. lherzolite: Till et al. 2012a vs. olivine + orthopyroxene in residue: Lee et al. 2009). In addition, there are a multitude of methods for reconstructing the volatile content of primary arc liquids, specifically the H_2O content (e.g., Sisson and Grove 1993; Baker et al. 1994; Wade et al. 2008; Kelley et al. 2010; Ruscitto et al. 2010; Waters and Lange 2015; Mitchell and Grove 2015), which has a significant effect on the pressure and temperature returned by thermobarometry. As a result, a direct comparison of existing thermobarometric estimates is problematic.

To provide a global-scale comparison, this paper compiles the results of published studies of mantle-melt thermobarometry conducted on erupted natural primitive arc lavas, tephras, matrix glass compositions, and melt inclusions. The methods used in these studies are reviewed, such that the effect of the methodology on the calculated pressure and temperature can be quantified and potential pitfalls identified. These results are then used to recommend a series of best practices for calculating primary liquid compositions from erupted primitive magmas and conducting the associated thermobarometry. These best practices are subsequently applied to a subset of the published primitive arc rock and melt inclusion compositions where there is adequate information in the source publication to carry out the recommended methods. These recalculated pressures and temperatures are then used to address overarching questions in arc magma genesis, such as the processes that govern the production of the most common types of primitive arc magmas, as well as provide observational constraints on the thermal structure and melt flow in the mantle wedge below arcs.

Literature review

A literature review of primitive arc liquid thermobarometry is presented here and restricted to thermobarometry that provides constraints on the mantle origin and evolution of arc magmas. Primary magmas are melts that have not been chemically modified in any manner since they segregated from their source region. In reality, all magmas experience some processing en route to the surface, which consists of crystal growth (fractional crystallization) and/or mixing of the magma with new materials (assimilation) or other magmas (magma mixing or recharge), such that they are instead called primitive magmas. The *P-T* constraints reviewed here are from natural primitive magmas or melt inclusions generated in the mantle wedge in the range between arc fronts and back-arcs.

Two methods of constraining the pressures and temperatures using natural primitive arc magmas are included in this literature review of mantle-melt thermobarometry (Fig. 1). The first method is thermometric and barometric calculations for primitive arc-related magmatic liquids, where bulk rock, matrix glass, or melt inclusion compositions are used with thermobarometers such as Mitchell and Grove (2015), Till et al. (2012a), Lee et al. (2009), Putirka et al. (2007), or Putirka (2008) following calculations to reverse fractional crystallization, post-entrapment crystallization etc. These studies are designed to calculate the temperature and pressure at which the liquid was in equilibrium with a peridotitic mantle (rather than the pressure or temperature of crystal fractionation, for example). The second method of constraining primitive liquid pressure and temperature in the literature compilation is experimental location of the multiple saturation points for primitive arc magmas. For these cases, a primitive magma or a synthetic oxide mixture of the same composition is used as the starting composition to determine the phase relationships for this sample over the portion of pressure-temperature space relevant to the upper mantle below volcanic arcs. The mineral phase boundaries are thus located, such that the point in pressure-temperature space where a melt is in equilibrium with a peridotitic mineral assemblage at given H_2O content, or the multiple saturation point, can be determined. These experiments are also used to calibrate many of the thermobarometers used in the first method. For the types of experiments covered in this review, the peridotitic assemblages at the multiple saturation point are either lherzolitic [olivine + clinopyroxene + orthopyroxene + aluminous phase (plagioclase, spinel, garnet)] or harzburgitic (olivine + orthopyroxene).

Thermobarometric studies in the literature were filtered for inclusion in this compilation with the following requirements: (1) that the samples used for thermobarometry were natural rock compositions erupted in an arc past or present, (2) that the samples were "primitive" as identified by the authors, and (3) that their pressure and temperature of melting or melt segregation from the mantle (or melt entrapment in the case of melt inclusions) were estimated with thermobarometry or experimentation (Table 1). The samples used for mantle-melt thermobarometry in these studies have a wide compositional variation, wider than what is usually considered primitive (Fig. 2) as no filters based on composition were applied for inclusion in the literature compilation in Figure 1. The source publications for melt inclusions with <57 wt% SiO_2, Mg# > 0.5, and locations from arc settings

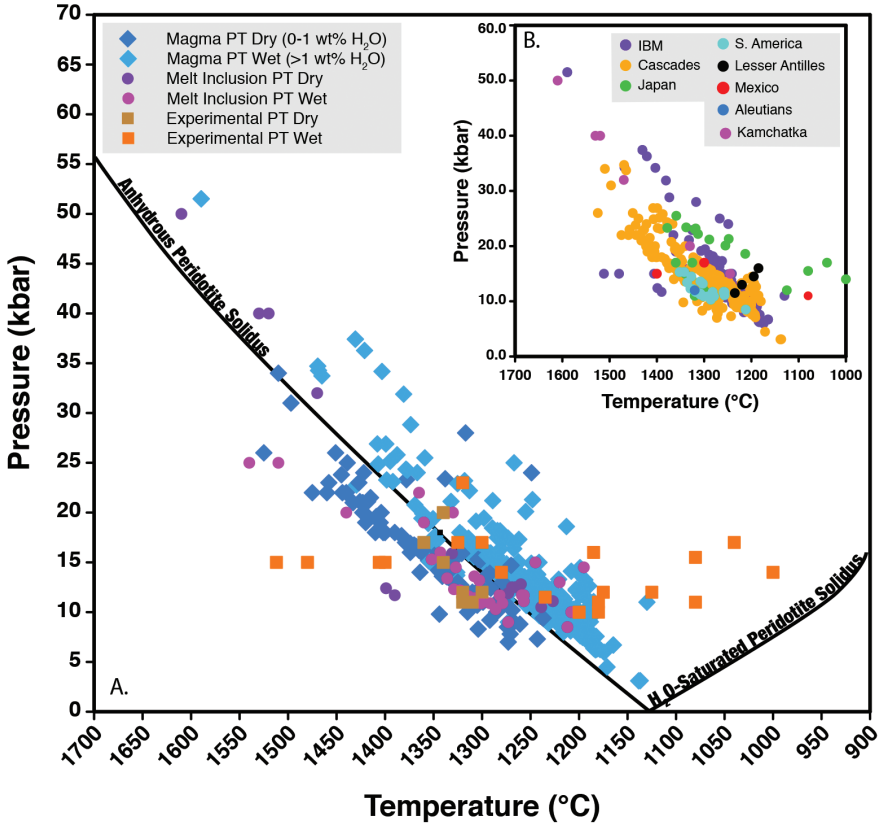

FIGURE 1. Compilation of primitive arc magma thermobarometry in the literature. The pressure and temperatures compiled here were calculated for primitive arc liquids by the studies listed in Table 1. The points are color-coded based on the technique used by each study to calculate the temperature and pressure of origin in the mantle and the water content. The anhydrous peridotite solidus is from Hirschmann (2000) and the H_2O-saturated peridotite solidus from Till et al. (2012b). Inset is same plot color coded according to subduction zone where each sample is found. The bulk of the data are from three subduction zones: 410 are from the Cascades, 131 are from the Izu-Bonin-Marianas and 21 are from Japan (n = 638 total).

in the GEOROC database were also queried for studies that met the criteria listed above. This review only includes melt inclusion pressure-temperature studies where the author identified the melt inclusion composition as reflecting a primitive liquid composition and both a temperature and pressure of mantle melt equilibration were determined. A few of the samples in the Cascades have been utilized for pressure-temperature determinations by multiple studies, and are represented as distinct points for each study in the literature compilation in Figure 1, such that not every plotted point is a unique sample. In total the literature compilation includes 638 independent estimates of the temperature and/or pressure of melt segregation for natural primitive arc magmas from 35 references (Table 1; Supplemental[1] Table 1).

Published thermobarometric estimates for primitive arc magmas and melt inclusions compiled directly from the literature vary between ~6–50 kbar and ~1000–1600 °C (n = 638) (Fig. 1; Supplemental[1] Table 1). The Cascades (n = 410) and Izu-Bonin-Marianas (IBM) (n = 131) arcs have the largest number of samples investigated to date and span the complete range of pressures and temperatures in the literature compilation with the exception of several experimental samples from Japan that suggest lower temperatures of mantle equilibration (<1150 °C).

REVIEW OF THE METHODS FOR MANTLE-MELT THERMOBAROMETRY IN THE LITERATURE COMPILATION

Here the methods employed to arrive at the pressure-temperature estimates in Figure 1 are reviewed to quantify the effect of different methodologies and identify best practices for an internally consistent set of new pressure-temperature calculations (presented in "Recalculation of pressures and temperatures for common arc magma types" section below).

Calculating the primary liquid composition through reverse fractional crystallization

To obtain the *P-T* conditions of mantle partial melting, a melt inclusion, bulk rock, or matrix glass composition first must be adjusted for crystal fractionation, until it is in equilibrium with an assumed mantle olivine composition and/or mantle mineral assemblage (i.e., lherzolite, harzburgite, or dunite). In addition, calculations to adjust for post-entrapment crystallization and/or diffusion may be necessary to return the composition of primitive melt inclusions to their original primary composition.

The fractional crystallization paths of mid-ocean ridge basalts (MORB) have been well-established through experimental and petrologic studies (e.g., Tormey et al. 1987; Grove et al. 1992; Yang et al. 1996). MORBs tend to fractionate olivine and plagioclase and the critical variable in reconstructing fractionation paths is pressure. Calculations to adjust for fractional crystallization become more complex for primitive arc magmas and other primitive magmas erupted in continental settings, as their phase assemblages and sequences of crystallization are dependent on other variables besides pressure. The key is to have a set of lavas

[1]Deposit item AM-17-55783, Table 2 and Supplemental Materials. Deposit items are free to all readers and found on the MSA web site, via the specific issue's Table of Contents (go to http://www.minsocam.org/MSA/AmMin/TOC/2017/May2017_data/May2017_data.html).

TABLE 1. Published studies that include arc mantle-melt thermobarometry compiled in Figure 1

Study	*P-T* method	*P-T* methods citation	H_2O estimate	H_2O effect on *P-T* citation
Anderson (1974)	Melt inclusion An-Fo-Di-liq/An-En-Di-liq thermobarometry	Bowen and Schairer (1935); Hamilton and Anderson (1976); Osborn and Tait (1952); Yoder and Tilley (1962)	Estimated by difference from electron probe analyses with Hawaiian reference standard	Bowen and Schairer (1935); Hytonen and Schaireer (1961); Yoder and Tilley (1962); Hamilton and Anderson (1967)
Baker et al. (1994)	Experiments on natural primitive magmas	NA	NA	NA
Bartels et al. (1991)	Experiments on natural primitive magmas	NA	NA	NA
Bouvier et al. (2008)	Melt inclusion comparison to experiments	Pichavant and Macdonald (2007)	Measured in Ol-hosted MI by ion microprobe	Comparison to experiments of Pichavant et al. (2002) and Pichavant and Macdonald (2007)
Draper and Johnston (1992)	Experiments on natural primitive magmas	NA	NA	NA
Elkins-Tanton et al. (2001)	Thermobarometry of primary liquids	Kinzler and Grove (1992)	–	–
Falloon and Danyushevsky (2000)	Experiments on primitive melt inclusion compositions and refractory mantle	NA	NA	NA
Gamble et al. (1990)	Comparison of primitive magmas to expts	Walker et al. (1979)	–	–
Grove et al. (2003)	Experiments on natural primitive magmas	NA	NA	NA
Hesse and Grove (2003)	Experiments on natural primitive magmas	NA	NA	NA
Kamentsky et al. (1995)	Melt inclusion comparison to experiments and adiabat T estimates	Ford et al. (1983) crystallization temperature extrapolated along an adiabat (3°/kbar) to a P determined from comparison to expts.	Measured in Ol-hosted MI by ion microprobe	Danyushevsky et al. (1992)
Kelley et al. (2006)	Matrix glass primary liquid thermobarometry	Langmuir et al. (1992)	Compilation with filtered and corrected H_2O	Calculated in this reference
Kelley et al. (2010)	Melt inclusion primary liquid thermobarometry	Lee et al. (2009); Langmuir et al. (2006); reformulation of Katz et al. (2003)	Measured in situ (FTIR, SIMS)	Langmuir et al. (2006) reformulation of Katz et al. (2003)
Kimura et al. (2006)	Barometry of primary liquids	pMELTS	Comparison to Experimental LLD	Sakuyama (1983)
Kimura et al. (2010)	Thermobarometry of primary liquids	Arc Basalt Simulator 3	Arc Basalt Simulator 3	Kimura et al. (2010)
Kimura et al. (2014)	Thermobarometry of primary liquids	Arc Basalt Simulator 4	Arc Basalt Simulator 4	Kimura et al. (2014)
Kohut et al. (2006)	Melt inclusion olivine-liquid thermometry and CPX-liquid barometry	Ford et al. (1983) and Putirka et al. (1996, 2003)	Measured in Ol-hosted MI by FTIR	–
Kushiro and Sato (1978)	Experiments on natural primitive magmas	NA	NA	NA
Lee et al. (2009)	Thermobarometry of primary liquids	Lee et al. (2009)	Assumed Cascades all 3 wt% H_2O, IBM all 7 wt% H_2O	Lee et al. (2009)
Leeman et al. (2005)	Olivine-liquid thermometry and primary liquid barometry	Sugawara (2000); Albaréde (1992) (with *P* correction from this study)	Qualitative comparison to experiments	–
Leeman et al. (2009)	Olivine-liquid thermometry and primary liquid barometry	Sugawara (2000); Albaréde (1992) (with *P* correction from this study)	Limited MI measurement + comparison to experiments	Putirka (2005)
Li et al. (2013)	Thermobarometry of primary liquids	Arc Basalt Simulator 3	Inferred from best fit models	Kimura et al. (2010) (which uses Katz et al. 2003)
Mullen and McCallum (2014)	Olivine-liquid thermobarometry and comparison to experiments	Putirka et al. (2008)	Lange et al. (2009) hygrometer	Putirka (2008)
Mullen and Weis (2015)	Thermobarometry of primary liquids	Lee et al. (2009)	–	–
Pichivant et al. (2002)	Experiments on natural primitive magmas	NA	NA	NA
Portnyagin et al. (2007, 2008)	Melt inclusion primary liquid thermobarometry	Katz et al. (2003)	Measured in Ol-hosted MI by ion microprobe	Katz et al. (2003)
Rowe et al. (2009)	Melt inclusion olivine-spinel thermobarometry	Balhause et al. (1991)	–	–
Ruscitto et al. (2010)	Melt inclusion primary liquid thermobarometry	Lee et al. (2009)	FTIR	Lee et al. (2009)
Sobolev and Danyushevsky (1994)	Melt inclusion comparison to experiments	Ford et al. (1983) extrapolated along liquidus (5°/kbar) to a *P* determined from comparison to expts.	Measured in Ol-hosted MI by ion microprobe and corrected for post-entrapment crystallization	comparison to experiments of Green (1973, 1976) and Kushiro (1990)
Tatsumi et al. (1983)	Experiments on natural primitive magmas	NA	NA	NA
Tatsumi (1981)	Experiments on natural primitive magmas	NA	NA	NA
Till et al. (2013)	Thermobarometry of primary liquids	Till et al. (2012)	Till et al. (2012)	Till et al. (2012)
Watt et al. (2013)	Melt inclusion primary liquid thermobarometry	Lee et al. (2009)	Measured in Ol-hosted MI by ion microprobe	Lee et al. (2009)
Weaver et al. (2011)	Experiments on natural primitive magmas	NA	NA	NA
Weber et al. (2011)	Experiments on natural primitive magmas	NA	NA	NA

related by fractional crystallization that can be used to identify: (1) the proportion of the phases that crystallized; (2) the degree of crystallization of the magma with a given phase assemblage; and, if applicable, (3) the switching point between sets of co-crystallizing phase assemblages (i.e., when the magma leaves a cotectic) (see full review of reverse fractionation methods in the Supplemental materials[1]). An alternative approach is to restrict thermometry and barometry to primitive samples that have experienced a minimal amount of crystal fractionation, such that they have only experienced olivine crystallization, which is more straightforward to adjust for. For example, for MORB, FeO* increases and CaO drops sharply when plagioclase joins olivine and a plot of FeO* or CaO vs. MgO can reveal samples that fall on an olivine control line vs. those that experienced multiphase fractionation.

Failure to adequately approximate the fractionation path, and in particular ignoring the requirement of the final liquid plotting on a mantle multiple saturation point, can have a significant effect on the adjusted liquid composition and thus the calculated source pressure and temperature. For example, if a polybaric, near fractional MORB primary melt experienced multiphase fractionation (olivine, followed by olivine + plagioclase) but is then adjusted for olivine-only fractionation, the calculated "primary melt" has artificially high MgO + FeO* and low-Al_2O_3 contents and thus the calculated mantle conditions are 100–150 °C hotter and up to 13 kbars higher than the actual pressure and temperature of generation for the parental MORB melt [see Fig. 6 of Till et al. (2012a) for a worked example]. A variety of approaches to reverse fractionational crystallization have been used for the primitive liquids with thermobarometry in the literature collected in Figure 1, with the dominant approach being the addition of only olivine back to the liquid composition.

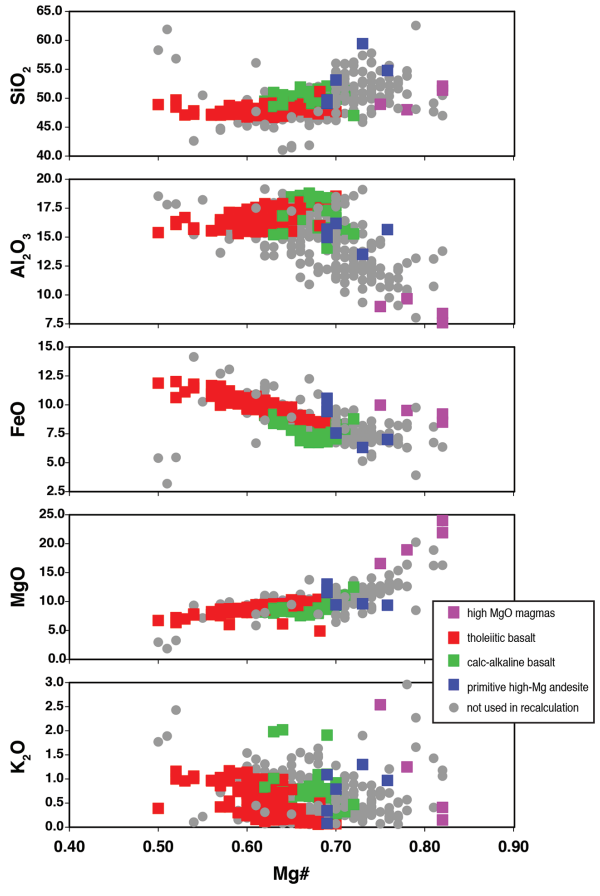

FIGURE 2. Harker diagrams. Compositions of primitive arc samples taken directly from studies in Table 1 and Figure 1, all of which are reported prior to reverse fractional crystallization calculations or any post-entrapment crystallization corrections in the case of melt inclusions. Samples with red, blue, green, and pink colored symbols were used for the new pressure and temperature calculations.

H_2O also plays an important role in calculations to reverse fractionational crystallization as it affects the order and composition of the fractionating phases. The body of work on arc magma fractionation paths suggests that the onset of plagioclase crystallization is the most important variable controlling the liquid line of descent of arc magmas. Experimental studies of the liquid line of descent illustrate that increasing the water contents at a constant pressure will cause the temperature of plagioclase crystallization to go down relative to the liquidus, thereby reducing the proportion of plagioclase crystallized compared to the ferromagnesian silicates and increasing the SiO_2 content of the residual liquid, as well as the relative temperature of magnetite or FeTi oxide crystallization (e.g., Sisson and Grove 1993; Grove et al. 2003; Hamada and Fujii 2008; Tatsumi and Suzuki 2009; Parman et al. 2011; Blatter et al. 2013). Although H_2O suppresses plagioclase crystallization at any oxygen fugacity, the amount of H_2O required to evolve the liquid to a calc-alkaline composition increases as oxygen fugacity decreases. Thus increasing the H_2O content at a given f_{O_2} drives the liquid more directly to the calc-alkaline field, essentially decreasing the concavity of the fractionation path as demonstrated in experimental studies such as Hamada and Fujii (2008) and summarized in Figure 3. Sulfur degassing can also cause a liquid to become more reduced during ascent (Anderson and Wright 1972; Kelley and Cottrell 2012; Moussallam et al. 2014), which alters the Fe^{2+} content appropriate for the primary melt temperature and pressure calculations (Brounce et al. 2014). The composition of the minerals that crystallize from hydrous magmas also change, for example the Ca/Na of the feldspar varies as a function of melt H_2O content (e.g., Sisson and Grove 1993), which will affect the thermobarometers that consider Ca and Na contents.

Although the theory for reverse fractional crystallization calculations for MORB and nominally anhydrous arc basalts discussed above still applies to wetter primitive arc magmas, there is not a well-accepted parameterization for the cumulative changes H_2O causes in the liquid line of descent. The cutoff H_2O content above which MORB-like fractionation paths no longer apply is not clear, but MORB-like fractionation schemes are likely most applicable over the range of H_2O contents relevant for MORB genesis and the higher the magmatic H_2O content, the more fractionation behavior will deviate from MORB-like behavior. Kimura et al. (2014) and Kimura and Ariskin (2014) are the only studies in the literature review in addition to the experimental studies on primitive arc magma pressures and temperatures that adjust the composition of the fractionating phases according to H_2O content. Therefore, future work is required to parameterize the discrete effects of H_2O during fractionation,

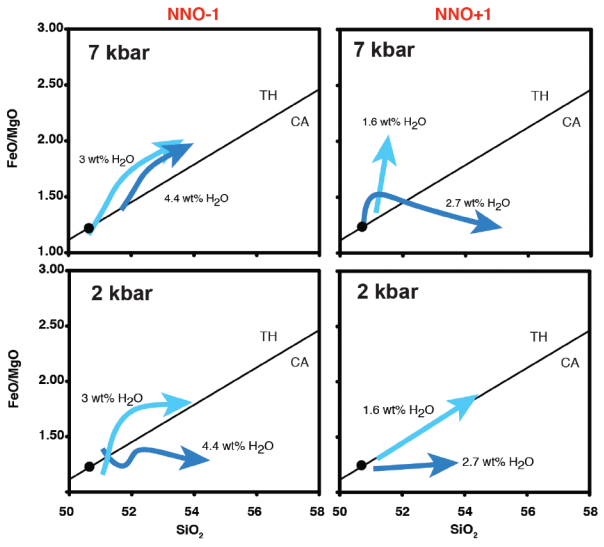

FIGURE 3. Summary of the liquid line of descent for a hydrous calc-alkaline basalt. Arrows represent the liquid lines of descent for high-MgO basalt following olivine fractionation at different conditions based on the experiments of Hamada and Fujii (2008). The bottom two plots represent experiments conducted at 2 kbar, and the top two illustrate experimentally determined liquid evolution at 7 kbar. Dark blue arrow represents experiments with the higher H_2O content in each plot. Comparison amongst the four plots illustrates differences in the liquid line of descent due to changes in oxygen fugacity, H_2O content, and pressure.

such that we can ultimately calculate hydrous primary arc magma compositions accurately.

Calculating pressure and temperature using primary magma compositions

Many experiments have demonstrated that the composition of the melt in equilibrium with a mantle peridotite (lherzolite or harzburgite) varies as a function of pressure, temperature, mantle source composition, and volatile content (e.g., Tatsumi 1981; Takahashi and Kushiro 1983; Kushiro 1990; Kinzler and Grove 1992a; Parman and Grove 2004; Gaetani and Grove 1998; Till et al. 2012a; Grove et al. 2013; Mitchell and Grove 2015). Thus primary liquid compositions can be used as a purely empirical geothermometer as long as the appropriate restrictions in bulk composition and saturating phases are made (Helz and Thornber 1987; Grove and Juster 1989). It follows that the temperatures and pressures reported in the literature (Fig. 1) are a function of the models that were used to calculate them. A full review and evaluation of the different thermometers and barometers that have been applied to calculated primary arc magmas is beyond the scope of this study [the reader is referred to existing reviews of thermometers for volcanic rocks in Putirka (2008) and for melts in equilibrium with a harzburgite in Mitchell and Grove (2015)]. Instead here the focus is to determine the spread of temperatures and pressure in the literature compilation attributable to the use of different thermobarometers, as well as make recommendations regarding the most reliable thermobarometers for primitive arc liquids.

The spread of temperatures that can be attributed to the choice of thermometer alone is on the order of ≤75 °C overall, and more likely to be ≤35–40 °C in most cases (see Supplemental Materials[1]). Recently published thermometers calibrated on the largest and most robust databases of experiments such as Putirka (2008) (their Eq. 4), Lee et al. (2009), and Till et al. (2012a) tend to agree to within 35 °C on average, which is within the error of these thermometers [see Putirka = 52 °C; Lee = ~40 °C (3%); and Till = 11 °C]. These three thermometers also include a term to consider the effect of H_2O, which makes them the most reliable and practical for the application to the continuum of dry to wet arc magmas at present. However, Lee et al. (2009) explicitly states that their melt barometer is "not intended for hydrous, unusually fertile or depleted mantle compositions that might characterize subduction-modified mantles" because it is based on the activity of SiO_2 in the melt, which varies with source mineralogy and water content, as well as pressure. Therefore although calibration of Lee et al. (2009) utilized a wide range of ultramafic melt equilibria experiments where olivine and orthopyroxene were stable in the residue, it is not well suited to melt generated in the garnet stability field, as the relationship between melt SiO_2 and pressure diminishes above ~2.5 GPa when garnet is present in the residue (T. Plank, personal communication, 2014), nor water-saturated systems, which also alter the silica activity of the melt. Till et al. (2012a) and Grove et al. (2013) are updated calibrations using the methodology of Kinzler and Grove (1992b), which require a lherzolite residue [plagioclase or spinel lherzolite for Till et al. (2012a), and garnet lherzolite for Grove et al. (2013)] but have the additional advantage over Kinzler and Grove (1992a) of being calibrated to consider metasomatized as well as variably depleted lherzolite. These lherzolite thermometers reproduce experimental liquids with the smallest average absolute errors of all the thermometers examined, only 11 °C for Till et al. (2012a) and 24 °C for Grove et al. (2013), and are thus extremely well suited to application in arc environments, provided the liquid appears to be in equilibrium with a lherzolite residue.

In the case where primary arc liquids are in equilibrium with $Fo_{90–91}$ olivine but are not in equilibrium with a lherzolite residue (e.g., Figs. 4b and 4c), the liquids may instead be saturated with a harzburgite or dunite residue, natural examples of which are found in exhumed sub-arc mantle sections and xenoliths (e.g., Kelemen et al. 1995; Pearce and Parkinson 1993; Morishita et al. 2011; Pirard et al. 2013). How to identify liquids in equilibrium with each of these potential residues is discussed in the Supplemental material (see Supplemental[1] Figs. 1 and 2). Mitchell and Grove (2015) developed a thermobarometer similar to Till et al. (2012a) and Grove et al. (2013) but specifically for primitive liquids in equilibrium with harzburgite residues. The Lee et al. (2009) and Putirka et al. (2007) thermometers significantly underpredict the temperatures of experimental melts in equilibrium with harzburgite compared to Mitchell and Grove (2015) and Till et al. (2012a), which are within error. With the addition of water to the melt, the thermometers of Till et al. (2012a) and Mitchell and Grove (2015) continue to be within error of the experimental temperature, whereas the Lee et al. (2009) and Putirka et al. (2007) are ~100 °C hotter. Several thermometers based on olivine-liquid equilibria exist, including a new model that includes the effect of oxygen fugacity by Putirka (2016), which can be used for liquids in equilibrium with dunite.

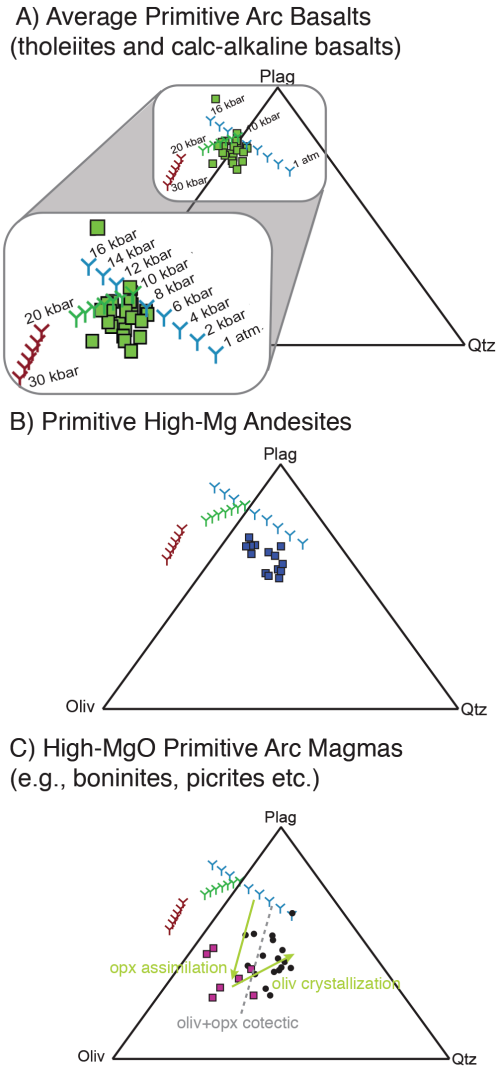

Figure 4. Pseudo-ternary projections for representative arc calc-alkaline and tholeiitic arc basalts, primitive andesites, and high-MgO liquids. (**a**) Pseudo-ternary projections depicting the compositions of representative tholeiitic and calc-alkaline arc basalts prior to reverse fractional crystallization calculations. These samples are shown along with the location of a melt in equilibrium with plagioclase (blue Y's), spinel (green Y's), and garnet (red Y's) lherzolite, also known as the lherzolite "multiple saturation points," over a range of pressures from Till et al. (2012a) and Grove et al. (2013), which are plotted in all three diagrams. These liquids in **a** are relatively silica-understaturated and plot towards the plagioclase apex because they originated from a lherzolite residue. (**b**) Pseudo-ternary projections depicting the compositions of representative primitive arc andesites and (**c**) high-MgO arc magmas such as boninites and picrites illustrated prior to any reverse fractional crystallization calculations. Overall both the liquid types in **b** and **c** are relatively silica-saturated and have a comparatively lower plagioclase component relative to the more typical arc basalts because they are in equilibrium with a more depleted mantle residue (i.e., harzburgite or in the case of a few high-MgO liquids dunite), rather than lherzolite. Samples plotted in all three figures are those used in the new calculations of pressures and temperatures with the exception of the black circles in **c** that are included to illustrate the range of high-MgO primitive arc magma compositions in the literature.

Differences in the assumed mantle f_{O_2} and thus the appropriate Fe^{2+} content of the primary melt will also affect the temperatures calculated. Although a range of approximately QFM-3 to QFM+2 has been estimated for the upper mantle (Frost and McCammon 2008 and references therein), and QFM to NNO for oceanic basalts (Putirka 2016), work on primitive arc magmas suggests a more oxidized range of oxygen fugacities (~QFM+1 to QFM+2 or even MH) is appropriate for the mantle in subduction zones (Brounce et al. 2014; Putirka 2016). The lower oxygen fugacities are thought to be found in drier/back-arc regions and the higher fugacities in the hydrated mantle due to the role of the subduction fluids/melts in oxidizing mantle wedge environments (e.g., Kelley and Cottrell 2009; Brounce et al. 2014).

The H_2O contents for samples included in the literature compilation in Figure 1 have been estimated using a range of techniques and this is likely the variable for which the quality of the constraints is the most heterogeneous. For example, some studies have carefully determined the H_2O content of each individual sample through ion probe or FTIR analyses of melt inclusions (e.g., Kelley et al. 2010; Ruscitto et al. 2010), where others utilized mineral chemistry and hygrometry (e.g., Mullen and McCallum 2014), or made comparison to experimental liquid lines of descent (e.g., Leeman et al. 2005, 2009; Kimura et al. 2009), and others choose to assign all samples from a given subduction zone the same water content (e.g., Lee et al. 2009). Even if the H_2O content of a primary melt has been effectively estimated, the calculated effect of this H_2O on mantle equilibration temperature and pressures differs between models and may vary systematically with melt compositions. The thermobarometers of Putirka et al. (2007), Lee et al. (2009), and Till et al. (2012a) include a calibration for the effect of H_2O on the calculated liquid temperature for lherzolite melts. The Till et al. (2012a) calibration results in the largest effect of H_2O on the liquid temperature, followed by Putirka et al. (2007) and then Lee et al. (2009). The temperature difference predicted by these models can be up to 67 °C at 5 wt% H_2O for a calc-alkaline basalt, which is greater than the uncertainty of these thermometers (further discussed in the Supplemental Materials[1]). The effect of H_2O on the liquid temperature can therefore introduce an equivalent or often larger spread in temperatures in the literature compilation than the choice of which thermometer was used (see Supplemental Materials[1]). The effects of H_2O on pressure are compared for the Lee et al. (2009) and Till et al. (2012) barometers in the Supplemental Materials[1]. The Lee et al. (2009) barometer has a larger model dependence on H_2O than Till et al. (2012a) and the calculated pressure of equilibration is 2.5 kbar (or ~8.5 km) higher with Lee et al. (2009) than Till et al. (2012a) for a calc-alkaline basalt with 5 wt% H_2O. This variability in the pressure calculations as a function of H_2O content is equivalent to or smaller than the range of pressures produced by using different barometers or types of reverse fractionation calculations on the same sample.

Thus large variations in pressure and temperature in Figure 1 may be attributed to different assumptions about H_2O content. And it follows that our ability to calculate the pressures and temperatures at which primitive arc magmas are sourced in the mantle and thus interpret mantle wedge processes is the most limited by the consideration of H_2O, specifically by differences in how the primary magmatic H_2O-contents are estimated (or

not), the lack of consideration of H_2O's effects on the reverse fractionation crystallization calculations in existing studies, and the differences between models for the effects of H_2O on mantle equilibration pressure and temperature.

Methods

A representative subset of the primitive arc samples with thermobarometry in the literature review in Figures 1 and 2 (n = 208 of 638 in literature review) were selected for a reassessment of their reverse fractional crystallization calculations and a recalculation of their pressures and temperatures of mantle equilibrium using an internally consistent set of methods and the latest thermobarometric tools that consider H_2O (Table[1] 2). Samples were chosen whose source literature provided substantial information about the sample's (or suite of samples) petrography and mineral compositions, oxygen fugacity, and where possible H_2O content. A wholesale recalculation for all samples used in the literature compilation is not possible because many source publications contain insufficient information to conduct the reverse fractionation calculations and/or estimate H_2O content. However, the samples included in the recalculation are representative of the full range of sample compositions in Figure 2 and calculated pressures and temperatures in the literature compilation in Figure 1. Once investigated the samples fall into three categories: (1) calc-alkaline basalts and low-K tholeiites; (2) primitive andesites; and (3) primitive boninites, picrites, and other high-MgO liquids (Figs. 4 and 5), and the methods for the recalculation of each category are discussed below (also see the worked example in the Supplemental[1] material). Here we distinguish high-MgO liquids with <52 wt% SiO_2 and >15 wt% MgO from primitive andesite with >52 wt% SiO_2 and <15 wt% MgO (avg. 9–10 wt% MgO). In addition, three samples appear to have formed in the presence of significant amounts of CO_2 or be the result of melting pyroxenite as demonstrated by their major element compositions projected onto pseudo-ternary [see diagrams in Figs. 9 and 11, respectively, and associated text in Grove et al. (2013)] and are excluded from the pressure-temperature calculations.

The subset of calc-alkaline and tholeiitic basaltic lavas or melt inclusions used for the recalculations are from the Cascade (Leeman et al. 2005; Rowe et al. 2009; Till et al. 2013), Lesser Antilles (Pichavant et al. 2002), and Mariana arcs (Kelley et al. 2010) and are similar to the majority of the rock types in the literature with pressure-temperature estimates. These samples tend to have experienced olivine, olivine + plagioclase, olivine + clinopyroxene, or olivine + plagioclase + clinopyroxene fractionation based on the mineralogy of the samples and/or the liquid compositions and required calculations to reverse between 4 to 26% crystallization (Fig. 6). These minerals were added back to the whole rock composition (usually in proportions reflecting the modal proportions in the sample), treating all Fe as FeO* and using partition coefficients appropriate for the H_2O contents of the sample (e.g., varying the Ca-Na plagioclase-liquid K_D as a function of H_2O) (see worked example in Supplemental[1] materials). The H_2O content of these samples were determined via SIMS or FTIR on melt inclusion or matrix glass by several studies and estimated using the methods listed in Table[1] 2 for the remaining samples. The major element compositions of these liquids are consistent with forming from a lherzolite residue, such that the reverse fractionation calculations aims at returning them to a lherzolite multiple saturation point and equilibrium with Fo_{90} mantle olivine (Fig. 4a). These adjusted primary liquids were used with the lherzolite thermometers and barometers of Till et al. (2012a) and Grove et al. (2013), which includes the effect of H_2O.

The subset of primitive andesites used for the recalculations are those studied in Mitchell and Grove (2015) and are from the Setouchi volcanic belt (Tatsumi and Ishizaka 1982; Tatsumi and Kushiro 1983), the Cascades (Baker et al. 1994; Grove et al. 2002; Mitchell and Grove 2015), Kamchatka (Bryant et al. 2010), and the Trans-Mexico volcanic belt (Weaver et al. 2011; Weber et al. 2011). These samples have high Mg# values (0.71–0.76) and their compositions are consistent with liquids in equilibrium with a harzburgite residue as predicted by the model of Mitchell and Grove (2015) without any reverse fractionation calculations (Figs. 4b and 5). Given the degrees of freedom, two of the three variables of pressure, temperature, and H_2O content can be calculated for these liquids using the thermometer, barometer and/or hygrometer for liquids in equilibrium with harzburgite from Mitchell and Grove (2015). Here the thermometer and hygrometer were employed and pressure was assumed based on the thickness of modern crust in these locations, which is on average 30 km (~10 kbar).

The subset of boninites, picrites, and other high-MgO magmas (>13.5 wt% MgO) used for the recalculations are dredge samples from the Bonin forearc (Li et al. 2013) and Mariana (Bloomer and Hawkins 1987), subaerial samples from the Marianas (Dietrich et al. 1978) and the New Britain arc (Cameron et al. 1983) and melt inclusions from the Tonga trench (Sobolev and Danyushevsky 1994) and eastern Kamchatka (Kamenetsky et al. 1995). They represent the samples with the highest Mg# values and high-MgO contents in the literature compilation (Fig. 2), as well as the samples that record the highest temperatures and pressures of mantle equilibration in the literature compilation (Fig. 1). Their high Mg# values of 0.74–0.82 suggest these liquids were in equilibrium with Fo_{90-94} olivine with a Fe-Mg K_D of 0.3 or that K_D values were higher than 0.3 to be in equilibrium with Fo_{90}

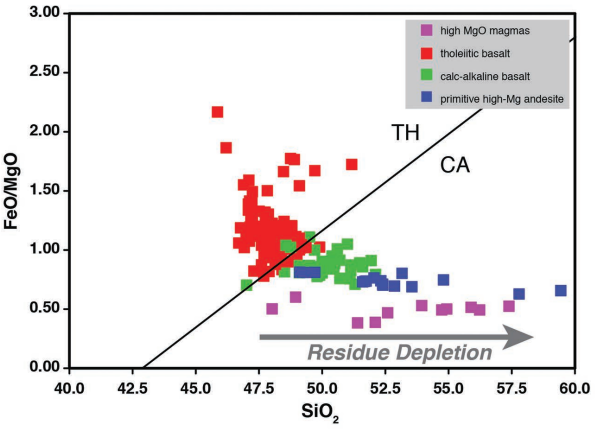

Figure 5. Recalculated primitive arc magma compositions. Composition of samples included in the new pressure and temperature calculations compared to the calc-alkaline vs. tholeiitic fields of Miyashiro (1974). Arrow indicates progressive depletion of the mantle residue that sources the primitive magmas (lherzolite > harzburgite > dunite).

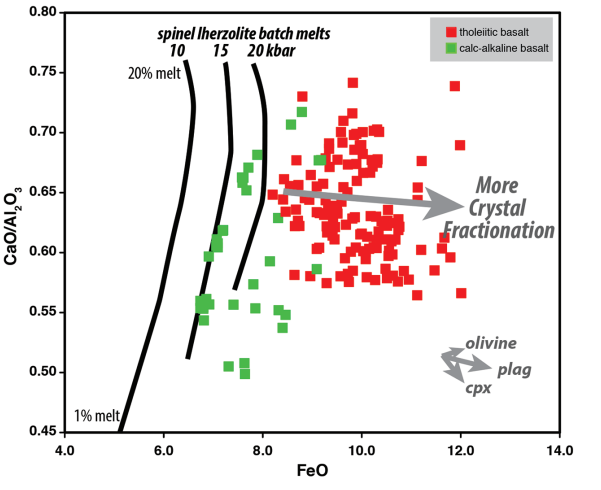

Figure 6. Comparative amount of crystal fractionation to be reversed prior to the new pressure and temperature calculations for the tholeiitic and calc-alkaline primitive basalts. Black curves represent the composition of 1–20% isobaric batch melts for a depleted Hart and Zindler (1986) mantle composition at 10, 15, and 20 kbar as predicted by the forward lherzolite melting model of Till et al. (2012a) as modified by Behn and Grove (2015). These curves illustrate the composition of primary nominally anhydrous melts prior to crystal fractionation. Crystal fractionation shifts the composition of these melts to the right along a vector whose direction is determined by the combination of olivine±plagioclase±clinopyroxene crystallization appropriate for that liquid. Samples on the right side of the plot have experienced more crystal fractionation than those on the left.

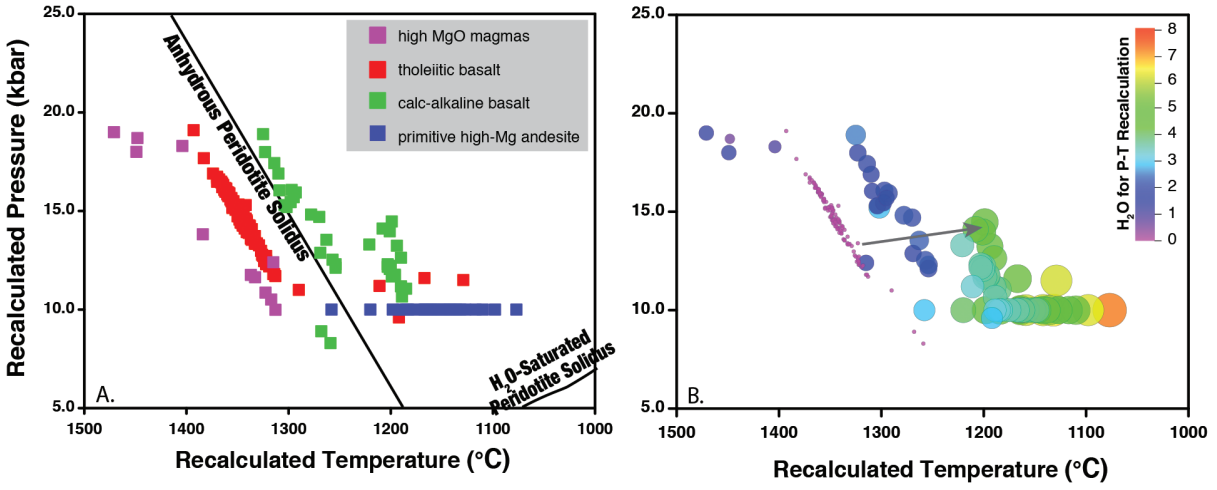

FIGURE 7. Recalculated temperatures and pressures with subset of the literature compilation. (**a**) Pressure-temperature plot color coded by primitive arc magma type. The new pressures and temperatures were calculated following internally consistent methods as described in the Methods section. The anhydrous peridotite solidus in **a** is from Hirschmann (2000) and the H_2O-saturated peridotite solidus from Till et al. (2012b). Pressures for the high-Mg andesites are all the same because the pressure was assumed to be that of the base of the av. arc crust (30 km, ~10 kbar on average) to accurately assess their temperatures of mantle equilibration using the Mitchell and Grove (2015) harzburgite-liquid hygrometer and thermometer. (**b**) Recalculated pressure and temperature contoured (by color and bubble size) for the H_2O contents (wt%) used in the recalculation. Samples in the recalculation are limited among other criteria to a range of representative compositions and to those with H_2O contents measured via SIMS or FTIR or adequate information to estimate H_2O via hygrometry with the exception of four tholeiites which are similar in composition to other nominally anhydrous tholeiitic magmas with H_2O estimates (see details in Methods for recalculations in Table[1] 2). Arrow illustrates the shift in *P-T* that results from estimating the *P* and *T* of the sample with 0 wt% H_2O (left) vs. 4.6 wt% H_2O (on the right at end of arrow).

olivine. As such, it was not necessary to adjust the liquids for fractionation to return these samples to equilibrium with the mantle. When plotted in pseudoternary space, these liquids exhibit lower plagioclase and clinopyroxene components than the mantle lherzolite multiple saturation points suggesting they may be in equilibrium with either a harzburgite or dunite residue instead (Figs. 4c, 5, and Supplemental[1] Fig. 2). As the liquids fall along the olivine-orthopyroxene saturation boundaries experimentally determined by Wagner and Grove (1998), they may be the product of either harzburgite melting or lherzolite melts that re-equilibrated with harzburgite in the lithosphere as they ascended (Grove et al. 2013; Wagner and Grove 1998). A few of the samples with the lowest clinopyroxene mineral component values plot in regions of liquids in equilibrium with a dunite (see Supplemental[1] Figs. 1 and 2) produced experimentally at very low melt-rock ratios (5–20% melt) at high temperatures 1220–1260 °C found in the hot core of the wedge (Mitchell and Grove 2016). Given the similarity of the majority of the high-Mg liquids to those in equilibrium with harzburgite, the Mitchell and Grove (2015) harzburgite thermometer and hygrometer were applied to all of them. For samples with H_2O contents measured via ion probe in melt inclusions or matrix glass, the measured values agree with those estimated via the Mitchell and Grove (2015) hygrometer.

RESULTS

The results of the recalculations show that the calc-alkaline and low-K tholeiitic basalitic samples were last in equilibrium with a lherzolite residue at intermediate pressures and temperatures of arc magma genesis between ~1130–1390 °C at 8.5–19 kbar at 0–6 wt% H_2O (Fig. 7). The primitive andesites were last in equilibrium with a harzburgite residue at intermediate to high-H_2O contents and represent the lowest temperatures and intermediate to low pressures of last equilibration between ~1075–1260 °C with H_2O contents of 3.2–7.2 wt% H_2O at 10 kbar. If pressures of last equilibration were in fact slightly higher at ~15 kbar, the liquids represent mantle equilibration temperatures of 1090–1270 °C at 6–10 wt% H_2O. The primitive boninites, picrites and other high-MgO liquids were last in equilibrium with a harzburgite residue on average and represent the highest temperatures over the entire range of pressures. Four of these samples are olivine-hosted melt inclusions (Kamenetsky et al. 1995; Sobolev and Danyushevsky 1994) and record temperatures of 1400–1450 °C at 18–19 kbar using the H_2O content of the melt inclusions determined by ion probe (0.60–1.4 wt% H_2O). The other seven high-MgO liquids, including boninite from the IBM arc (Bloomer and Hawkins 1987; Dietrich et al. 1978; Li et al. 2013), record shallower conditions of last mantle equilibration of 1310–1385 °C at 14–10 kbar at 1.0–1.6 wt% H_2O.

Overall the recalculated fractionation paths and thermobarometry yielded lower temperatures (ΔT = –1–198 °C, n = 166) than the published literature estimates with only a few samples from the Cascades yielding higher temperatures (ΔT = +22–327 °C, n = 7) (Table[1] 2). The recalculated pressures also tend to be lower than the literature values (ΔP = –1–21 kbar, n = 168) with a few being higher (ΔP = +0.5–19 kbar, n = 5). These lower temperatures and pressures largely result from using multiple phases that reflect the sample's mineralogy to adjust for fractional crystallization, as well as the use of modern thermobarometers for lherzolite and harzburgite residues (Till et al. 2012a; Grove et al. 2013; Mitchell and Grove 2015). This exercise reinforces the large effect of a reverse fractionational crystallization calculation scheme consistent with the rock mineralogy and H_2O content, as well as imposing the criteria that the major element composition of the fractionation-adjusted liquid match the composition of experimentally determined liquids in equilibrium with the appropriate mantle residue (e.g., lherzolite vs. harzburgite), in addition to the appropriate mantle olivine forsterite content. Because the recalculated samples included

those with the maximum and mininum pressures and temperatures reported in the literature, these recalculations suggest the range of pressures and temperatures recorded by primitive arc magmas is in fact much smaller than suggested in Figure 1. Instead arc primitive arc magmas likely only record last pressures and temperatures of equilibration between 1050–1450 °C at 8–19 kbar, rather than up to 1600 °C at 50 kbar as reported in the literature (Fig. 7).

Discussion

Now that an assessment of the variability in the literature compilation due to methodology has been made and a subset of the primary arc magma compositions have been used to recalculate their conditions of mantle equilibration using internally consistent methodology (hence forward referred to as the "recalculated compilation"), there is the opportunity to interrogate the new *P-T* calculations for what they reveal about the underlying mantle processes.

Mantle melting processes. In part, the pressure and temperature variations in the recalculated compilation are the result of the multiple mantle melting processes. The tholeiitic arc basalts are thought to be generated by adiabatic decompression melting of nominally anhydrous, hot mantle being advected into the mantle wedge during corner flow (e.g., Grove et al. 2002; Sisson and Bronto 1998). The calc-alkaline lavas on the other hand likely result from hydrous flux melting, where a slab-derived H_2O-rich component initiates melting at the vapor-saturated lherzolite solidus at the base of the mantle wedge and the buoyant melt ascends into the hot core of the mantle wedge (e.g., Grove et al. 2003; Till et al. 2012b). As it rises, this melt equilibrates with the hotter mantle, dissolving mantle minerals to increase the melt fraction and lower the melt H_2O-content. Based on the calculations of the likely mantle residue composition here and in previous studies, the high-MgO arc primitive magmas and primitive arc andesites are likely the result of these same processes causing melting of harzburgite rather than lherzolite.

Once the first melt is formed, the continuation of mantle melting can be represented by two end-member categories; that where there is equilibration between the melt and solid at all times so that the bulk composition is fixed (i.e., equilibrium or batch melting) and that where the liquids are extracted as soon as they form so that the bulk composition of the residual solid changes (i.e., fractional melting). The major and trace element composition of MORBs reveal that they are the product of polybaric near-fractional melting (e.g., Johnson et al. 1990; Langmuir et al. 1992) and record the average pressure and temperature of the mantle melting column (e.g., Kinzler and Grove 1992b). In contrast, several detailed studies suggest that anhydrous to damp primitive magmas erupted in arc settings appear to be the product of batch melting (e.g., Bartels et al. 1991; Bacon et al. 1997; Kent and Elliott 2002; Kelley et al. 2010; Till et al. 2012a), such that they only record the last pressure and temperature of equilibration with the mantle rather than the average pressure and temperature as in near-fractional melting. This hypothesis is further tested here using the forward mantle melting model of Behn and Grove (2015), which is built on the formulation of Kinzler and Grove (1992a, 1992b, 1993) and Kinzler (1997) for MOR-melting and incorporates new experiments from Till et al. (2012a) on metasomatized and depleted mantle melting so as to make the model appropriate for melting beneath arcs. Approximately 1–10% isobaric batch melting of a depleted Hart and Zindler (1986) mantle [HZ-Dep1 in Table 1a of Kinzler and Grove (1992b)] in the spinel lherzolite field at 10–20 kbar overall reproduces the major element composition of the calc-alkaline basalts used for the recalculations (Fig. 8b). The tholeiitic basalts with recalculated pressures and temperatures can be fit by incremental batch melting of the same mantle composition with 90% melt extraction at each step (i.e., near fractional melting) between 20–9 kbars, dF/dP of 1% per kbar and an adiabatic gradient of 1.5 °C per kilobar over a range of mantle potential temperatures between ~1450–1300 °C. They can also be fit by batch melting curves like those that fit the calc-alkaline basalts (Fig. 8a). Therefore the calc-alkaline basalts reviewed here, and perhaps also the tholeiitic basalts, record their last pressure and temperature of mantle equilibration (i.e., the conditions of melt extraction), not the initiation of melting. These equilibration conditions are commonly misinterpreted as indicating shallow and hot melting beneath arcs. Instead this interpretation reinforces prior observations by studies such as Kelley et al. (2010), Weaver et al. (2011), and Till et al. (2013) that primitive arc magmas tend to re-equilibrate near Moho depths as they rise from their deeper points of origin. This is further illustrated when the recalculated compilation is compared to geodynamics models of the temperature distribution within the mantle at modern subduction zones in the following section.

In the case of melt inclusions, the recorded temperatures and pressures reveal the conditions at which the primitive melt was trapped by the host mineral. For the majority of cases in this study the host mineral is olivine, with the remainder being clinopyroxene. Therefore, they record the pressures and temperatures during olivine or clinopyroxene crystallization. In the literature compilation and the recalculated compilation, the temperatures and pressures of melt inclusion formation overall appear to be similar to those where primitive magmas are extracted from the mantle.

Geodynamic models. Geodynamic models with increasing complexity have been applied to solid-state mantle convection in the mantle wedge. Vertical paths through a suite of modern models are compared to the recalculated magma thermobarometry in Figure 9. The recalculated pressures and temperatures for damp to wet magmas tend to match the thermal structure of the Kelemen et al. (2003) models, while those from the nominally anhydrous magmas reflect higher temperatures at a given pressure than predicted by any model. Kelemen et al. (2003) compared the much more limited set of petrologic constraints on the pressure-temperature conditions for arc magmas and sub-arc crust available at the time to existing geodynamic models, and geared their modeling efforts toward reproducing the natural observations.

The comparison of the recalculated magmatic pressure-temperature compilation to the thermal structures predicted by dynamic models suggest that the magmas experience thermal equilibration in the hottest shallowest nose of the mantle wedge before they are extracted (Fig. 10). Syracuse et al. (2010) predict maximum temperatures in the hot core of the wedge that vary between 1200 or 1275 °C (depending on the location of full coupling between the mantle and slab) to 1459 °C at different subduction zones with an average of ~1400 ± 54 °C. This suggests re-equilibration in the hot shallow nose of the mantle wedge at different arcs could lead

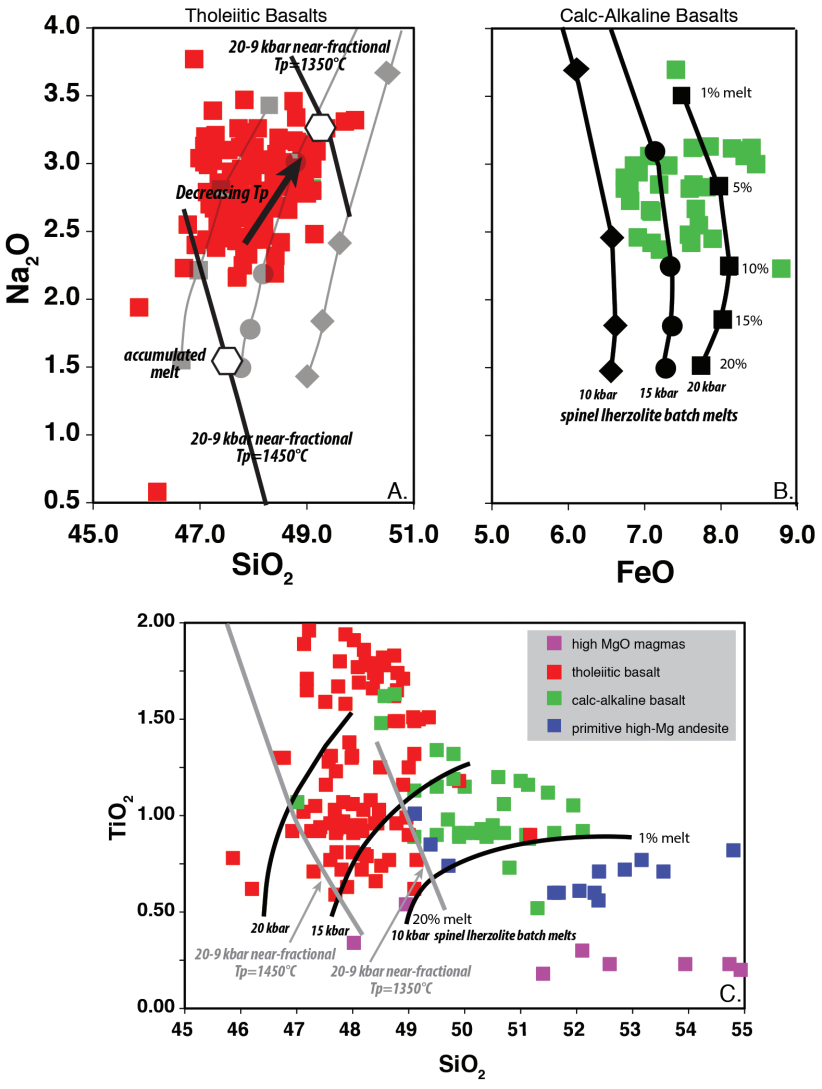

Figure 8. Comparison of arc basalts to forward modeling of batch vs. near-fractional mantle melting. (**a**) Comparison of tholeiitic basalts used for the pressure and temperature recalculations to incremental batch melts of a depleted Hart and Zindler (1986) mantle composition with 90% melt extraction and dF/dP = 1% per kbar and an adiabatic gradient of 1.5 °C per kbar using the forward mantle model of Till et al. (2012a) as modified by Behn and Grove (2015). Gray batch melting curves shown for comparison as described in **b**. (**b**) Comparison of the calc-alkaline basalts used for pressure and temperature recalculations to isobaric batch melting curves for a depleted Hart and Zindler (1986) mantle composition at 10, 15, and 20 kbar as predicted by the forward lherzolite melting model of Till et. al (2012a) as modified by Behn and Grove (2015). (**c**) Comparison of all rock types to the batch melting and near-fractional melts of spinel lherzolite. The calc-alkaline basalts are consistent with 1–10% batch melts of a depleted mantle at 10–20 kbar. The tholeiites can be modeled by either batch melting at average higher pressures and extents of melting or by near-fractional melting between 20–9 kbar.

to a natural variation in magmatic temperatures of ~200–250 °C. While the range of recalculated pressures and temperatures broadly match Syracuse et al. (2010), in some cases the magmas are warmer than the model predictions at specific arcs. For example, magmatic temperatures are as warm as 1400 °C below the Cascades and 1450 °C below the Kamchatka and Tonga arcs, while the model predicts maximum temperatures beneath Cascadia of 1285–1312 and 1300 °C below the Kamchatka and Tonga arcs. This may be in part due to the limitations of modeling mantle wedge thermal structures in two dimensions.

Shown for comparison in Figure 9 are the maximum pressure-temperature conditions for subduction zone blueschists and eclogites and thermal models for the subducting slab (Penniston-Dorland et al. 2015). The peak thermobarometric conditions recorded in exhumed metamorphic rocks are on average 100–300 °C warmer than the models, and the greatest discrepancies occur at <2 GPa. Penniston-Dorland et al. (2015) argue that the omission of significant shear heating (up to 250 °C at 35 km depth) and the exothermic hydration reactions within the overlying mantle just above the slab-wedge interface (<200 °C at 1 GPa for a flux of ~0.1 kg H_2O/m^2/yr from slab) are two of the most significant potential causes of this discrepancy. While the physics of heating up a slab are simpler than predicting the temperature of convecting mantle in the wedge, these features could also account for some of the discrepancy between the hottest primitive arc magma samples and the dynamic models. However the dimensionalization of temperature in the dynamic models and the prescribed boundary conditions are likely more significant factors controlling the discrepancies between the petrologic estimates and geodynamic models. For example, geodynamic models may underestimate the temperatures possible at the shallowest depths because of the prescribed lithospheric thickness in the models [e.g., 45–55 km for van Keken et al. (2002) and Kincaid and Sacks (1997)]. Results from Till et al. (2013) for the southern Cascadia subduction zone suggest the continental lithosphere must be ≤35 km thick. The observation that the warmer, driest arc basalts in the recalculated compilation require adiabatic decompression melting of asthenospheric mantle supports the interpretation that the convecting mantle extends to an average depth of ~30 km or less (~10 kbar) at arcs, even at arcs with an overriding continental plate.

In addition, strong focusing mechanisms that direct fluids and melts to hot and shallow regions beneath the arc may help explain the abundance of shallow, hot arc magmatic temperatures. Wilson et al. (2014) develop models that incorporate strong temper-

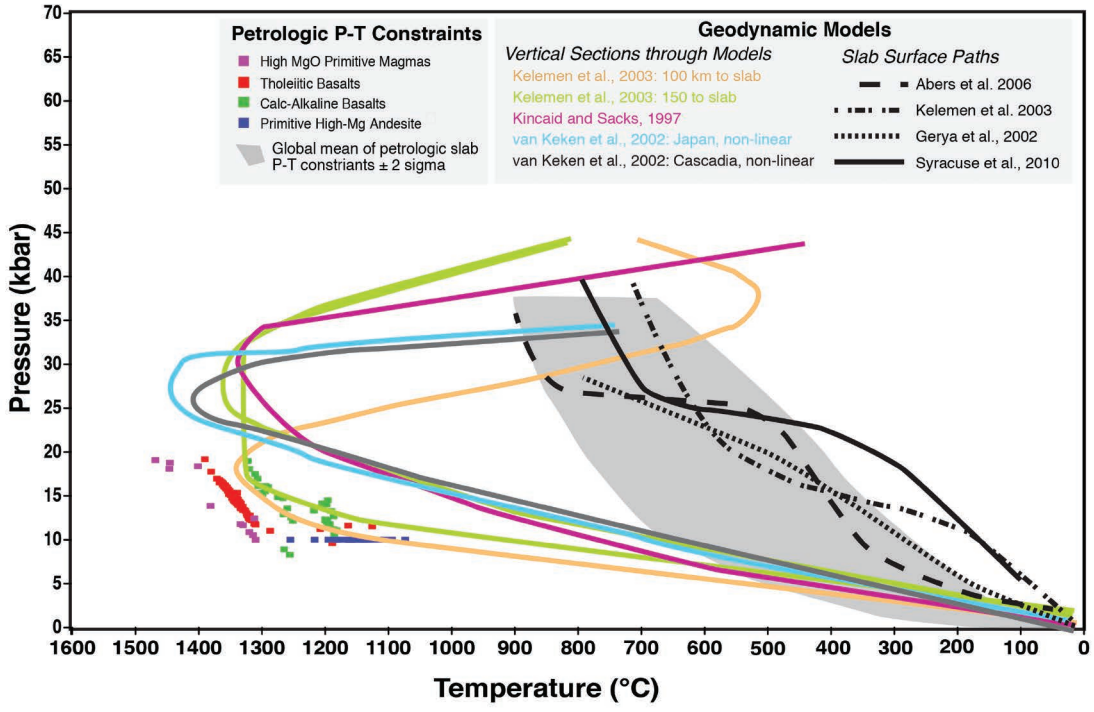

FIGURE 9. Comparison to geodynamic models. *P-T* paths from a selection of modern thermal models of subduction zones are compared to the thermobarometry data set. Colored lines represent the temperature conditions at vertical slices through the mantle wedge. The Kincaid and Sacks (1997) curve is from their model for fast subduction of a thin plate assuming a mantle potential temperature of 1400 °C. The van Keken et al. (2002) curve is from their models with a non-linear mantle viscosity and compares the structure of a "warm" (Cascadia) vs. "cold" (Japan) subduction zone. The Kelemen et al. (2003) curves compare slices through the model at two different distances from the trench, one closer to the trench where the slab is at 100 km depth (representing the hottest conditions at the shallowest depth from the models) and one further from the trench with the slab at depths of 150 km. Black solid and dashed lines are temperature conditions for the slab surface from a suite of relevant models compared to the gray field of thermobarometry constraints for the slab from exhumed metamorphic rocks as summarized in Penniston-Dorland et al. (2015). In both the magmatic thermobarometry reviewed here and the slab thermobarometry, the models tend to only reproduce the cooler petrologic observations.

ature-dependent rheologies in the slab and the wedge, and a physically reasonable model of fluid flow that includes the interaction of fluid transport with solid rheology in the form of compaction pressure. Similarly, Wada and Behn (2015) examine the effects of grain size on fluid flow in the mantle wedge. These models are able to reproduce the localization of fluids and melts to the subarc region with this more realistic permeability and solid viscosity structure. Although these models do not predict temperatures as warm as many of the magmatic temperatures in the recalculated compilation, they suggest a mechanism to explain the clustering of the *P-T* points at the shallowest pressures. These focusing mechanisms combined with the petrologic observations of shallow last conditions of mantle equilibration also provide an explanation for why wet and dry arc magmas are erupted in close spatial and temporal proximity at many arcs such as the Cascades (e.g., Till et al. 2013).

Melt-flow mechanisms. In addition to the various melting mechanisms for primitive arc magmas, the rising melt flow behavior also controls the ultimate pressure and temperature recorded. The maintenance of equilibrium between the melt and the mantle requires reactive porous flow as a mechanism for transporting the melts rather than diapiric or channelized flow (e.g., Navon and Stolper 1987; Grove et al. 2002). Reactive porous flow can be approximated as Darcy flow where permeability exerts the main control on the melt ascent rate and whether or not the melts can achieve thermal and chemical equilibrium. Provided permeability is sufficient for the fluids to outpace subduction, small degree batch melts will re-equilibrate with the hotter overlying mantle, dissolving silicate minerals and diluting the H_2O content as they rise (Grove et al. 2002). Alternatively, if melt flow occurs as diapiric or channelized flow, it can be approximated by Stoke's flow and the size of diapirs is the main control on whether thermal and chemical equilibration with the surrounding mantle will occur. Modeling suggests that for diapirs large enough to escape subduction flow, the ascent rate is too rapid for thermal equilibration with the surrounding mantle to occur (Grove et al. 2002).

Thermal gradients in the mantle wedge can be up to 30–40 °C/km based on geodynamic models (Cagnioncle et al. 2007; Syracuse et al. 2010). Therefore in the reactive porous flow model required for batch melting (Fig. 8), a difference in the pressure of last equilibration of 10 vs. 15 kbar (~15 km) equates to a difference in the temperature of last equilibration of up to 450 °C (Fig. 10). This difference in last equilibration conditions is similar to the difference between the coolest primitive andesites and the hottest boninites, including notably within the Kamchatka arc where these conditions are recorded within the same arc. Geochemical and isotopic modeling suggests >90% of the major element abundances in primitive hydrous arc magmas can be explained

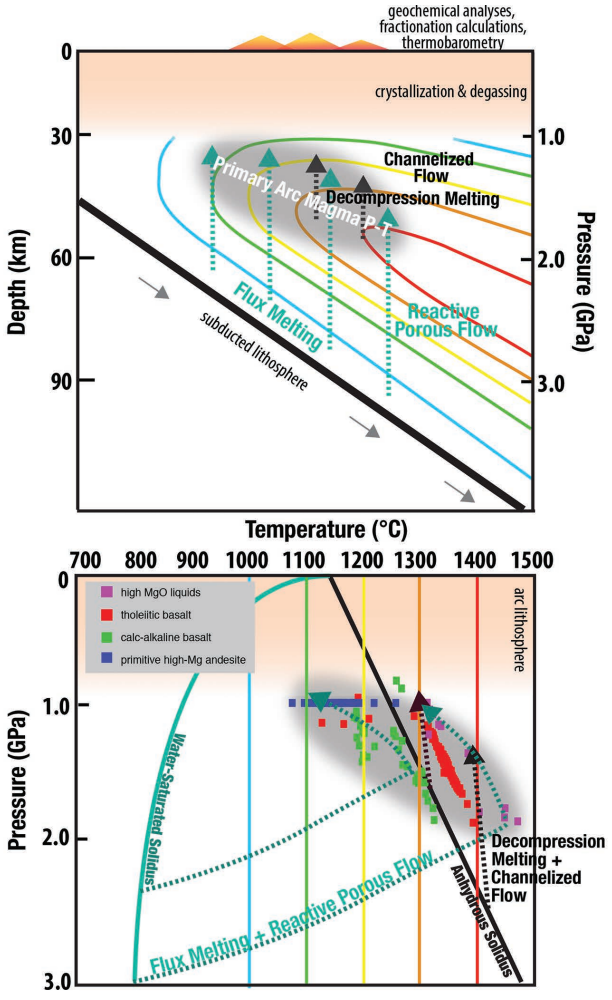

◀**Figure 10.** Summary of mantle processes that form primitive arc magmas reviewed in this paper. (**a**) 2D schematic cross section of subduction zone with isotherm locations from Kelemen et al. (2003). (**b**) Pressure-temperature diagram with the recalculated pressure and temperatures for primitive arc magma in Table[1] 2 shown in colored squares (which all fall within the gray field in panel (**a**). The anhydrous peridotite solidus is from Hirschmann (2000) and the H_2O-saturated peridotite solidus is from Till et al. (2012b). Hydrous arc magmas are first formed at the locations of the water-saturated mantle solidus just above the subducting lithosphere at pressures of ~20–30 kbar and then rise via reactive porous flow (teal dashed arrows) into the hot core of the mantle wedge where their melting extent increases and the water content decreases due to continued re-equilibration with the mantle. As they continue to rise into the cooler top portion of the mantle wedge via reactive porous flow their melt fraction decreases. The recalculated pressures and temperatures (gray field in **a** and **b**) reflect the conditions during their re-equilibration in the top half of the mantle wedge immediately prior to their extraction from the mantle. If hydrous magmas rise via channelized flow, they would record much lower temperatures at a given pressure than any magma in the recalculations done here or the literature compilation in Figure 1. When the mantle residue for this process is lherzolite, calc-alkaline basalts are generated. Alternatively, when the mantle residue is harzburgite, depending on the H_2O content either high-Mg andesites (higher average H_2O content, lower average temperatures) or high-Mg liquids (lower average H_2O content, higher average temperatures) are generated. Nominally anhydrous arc tholeiites are generated by near-fractional decompression melting at or near the anhydrous lherzolite solidus in the upwelling back limb of corner flow at ~20–10 kbar. These melts are focused into the same region of last mantle equilibration as the hydrous melts. Adiabatic ascent of these magmas (black dashed arrows) preserves the higher temperatures of their formation rather than the lower temperatures in the top half of the wedge. Some relatively dry high-Mg liquids may also be generated via this process when the mantle residue is harzburgitic.

as a product of flux melting and ascent via reactive porous flow (e.g., Grove et al. 2002), which is also supported by the composition of mantle xenoliths and field observations from the roots of arcs (e.g., Kelemen et al. 1992; Bouilhol et al. 2009). Therefore, a likely explanation for the calc-alkaline basalts and primitive andesites with temperatures lower than the anhydrous peridotite solidus is that these magmas re-equilibrate as they rise, and record the decrease in temperature during ascent out of the hot nose of the wedge (dashed teal ascent path in Fig. 10). Variability within the pressures and temperatures recorded by these hydrous magmas can be attributed to variations in subduction zone thermal structure through time, along strike, or between arcs.

Alternatively, if channelized flow and a fluid adiabat of 1 °C/km are assumed (Nisbet 1984), a 5 kbar difference in a magma's last pressure of equilibration equates to only a ~15 °C difference in the temperature. There is evidence that the incompatible trace element budget of hydrous arc magmas is contributed from a fluid and/or melt component present in the mantle that rises via adiabatic diapiric or channelized flow and does not re-equilibrate (e.g., Grove et al. 2002; Pirard and Hermann 2015). However, if a hydrous magma forms at or near the water-saturated solidus at 30 kbar, adiabatic ascent to 10 kbar would lower magmatic temperatures on the order of 60 °C and induce crystallization [see Grove et al. (2012), Fig. 2]. As no magmas in the recalculated compilation record temperatures of ≤1000 °C at any pressure, these magmas either crystallize before they reach the surface, or water-rich magmas do not rise via diapiric flow. Instead the recalculated compilation suggests adiabatic ascent may only be possible for the nominally anhydrous thoeliitic magmas (Fig. 8).

Models that include compaction pressure such as Wilson et al. (2014) represent an intermediate melt/fluid flow mechanism on the continuum between reactive porous and channelized flow models, which could also be responsible for intermediate temperature magma types. Alternatively, reactive porous flow may operate until there is a change in mantle permeability that causes a transition to channelized flow (e.g., Kelemen et al. 1997; Aharonov et al. 1997). Future work is required to determine if these hypotheses about melt flow are robust. The recalculated compilation provides a powerful set of pressure, temperature, and compositional observations to test any proposed model.

Summary of Thermobarometry and Mantle Origins for Four Types of Primitive Arc Magmas

Low-K tholeiitic arc basalts represent nominally anhydrous lherzolite melts and record high-average temperatures (~1300–1390 °C) between 10–20 kbar, which are generated by

adiabatic decompression melting in the back limb of corner flow (Fig. 10). These magmas tend to follow more tholeiitic liquid lines of descent in the crust similar to MORB's due to their low H_2O and more reducing f_{O_2}. Thus the appropriate reverse fractionation adjustment for these samples are the easiest to predict. These samples are the best suited to modern lherzolite thermobarometers (e.g., Till et al. 2012a; Lee et al. 2009; Putirka 2008) which yield temperatures of origin within 30 °C on average, making their pressures and temperatures of mantle equilibration the most reliable.

Calc-alkaline arc basalts record comparatively lower average temperatures (1100–1300 °C) over the same pressure interval due to melting lherzolite in the presence of higher H_2O contents (>1 wt%). The lower temperature samples at a given pressure likely represent melts generated at or near the H_2O-saturated solidus, which rise through the mantle via reactive porous flow (Fig. 10). Higher temperature calc-alkaline basalts (1250–1300 °C) may be the result of the same process or adiabatic ascent from an H_2O-undersaturated solidus due to lower H_2O contents. The higher H_2O and f_{O_2} of calc-alkaline basalts result in their more complex and variable fractionation paths in the crust. Thus caution is required when reverse-fractionating these samples and the more information about the suite of samples, their mineral contents, mineral compositions and H_2O contents, the better the chance of an accurate fractionation-adjusted composition. These samples are also appropriate for use with the lherzolite thermobarometers but will yield different results depending on the thermobarometer chosen because of the different calibrations for the effect of H_2O on their mantle equilibration pressure and temperature.

Primitive high-Mg andesites record the lowest temperatures at a given pressure in the recalculated compilation and are generated by 20–30% melting of harzburgite residue that has been enriched by alkalis during metasomatism over a range of H_2O contents (0–7 wt%). The primitive nature of the samples in the recalculated compilation is such that they do not require any reverse fractionation calculations to be in equilibrium with the mantle, although liquid lines of descent for these primitive rock types have been studied by Grove et al. (2003) and can be used to restore these samples to liquids in equilibrium with the harzburgite. The composition of harzburgite-derived mantle melts and their associated pressures, temperatures, and H_2O contents have been experimentally calibrated by Mitchell and Grove (2015). If these liquids are used with lherzolite thermometers or similar, they will yield higher temperatures, in error by up to 250 °C.

High-MgO arc magmas, such as boninites and picrites, record the highest temperatures for a given pressure in the recalculated compilation and their major element compositions are consistent with either harzburgite melting or lherzolite melts that re-equilibrated with harzburgite or dunite as they ascended (Grove et al. 2013; Wagner and Grove 1998; Mitchell and Grove 2016) at relatively low-H_2O contents. Their pressures and temperatures are consistent with thermal re-equilibration in the hottest nose of the mantle wedge and in some cases reactive porous flow to somewhat shallower conditions. These samples also tend to be so primitive that no reverse fractionation calculations are required to be in equilibrium with the mantle. Little to no experimental work has been done to constrain their fractionation paths. These samples will also yield a wide range of temperatures when used with lherzolite thermometers, which vary by almost 200 °C. The harzburgite thermobarometer of Mitchell and Grove (2015) appears to be the most appropriate given the composition of the liquids examined here, and yields temperatures at the lower end of the range.

Implications

The collection of published mantle pressure-temperature constraints from primitive arc magmas and the recalculations presented here provide observational constraints for shallow mantle processes at subduction zones relevant to various disciplines. For example, in addition to the petrologic and geochemical perspective on how much of the range of calculated magmatic pressures and temperatures at arcs is "real" and likely melt generation models, the recalculated compilation provides observational constraints for geodynamic models of the thermal structure and melt flow at subduction zones. The magmatic pressures and temperatures also provide the opportunity to further quantify the effect of melt on seismic velocity, attenuation, and electrical conductivity in the upper mantle below arcs and to continue to evolve three dimensional maps of melt distribution at subduction zones.

Several opportunities for future petrologic and geochemical study also arise. This paper focuses on the what can be learned from the major element composition of arc magmas and a logical next step is to interrogate the trace element and isotopic compositions of the magmas in the literature and recalculated compilation to further interrogate and differentiate between magmas formed by decompression melting and flux melting. As discussed in the review of reverse fractional crystallization calculations above, there is a need to develop robust parameterizations for the compositional effects of variable H_2O contents on the liquid line of descent for primitive arc magmas over the range of pressures and oxygen fugacities at which they crystallize in the arc lithosphere. In addition, the recalculated magmatic pressure-temperature compilation can ideally be used to understand the extent to which variations in the conditions of mantle equilibration can be attributed to variations between arcs with different subduction parameters (slab dip, convergence rate, etc.), as well as variations along strike within an arc.

Acknowledgments

Deep thanks are extended to K. Putirka for the invitation to participate in *American Mineralogist's* 100th anniversary, which precipitated this work. To T. Grove, A. Mitchell, and the EPIC group at ASU for many stimulating conversations along the way. To T. Sisson, K. Kelley, and K. Putirka for their constructive and insightful reviews of the manuscript. This work was supported by NSF grant EAR-1447342.

References cited

Abers, G.A., van Keken, P.E., Kneller, E.A., Ferris, A., and Stachnik, J.C. (2006) The thermal structure of subduction zones constrained by seismic imaging: Implications for slab dehydration and wedge flow. Earth and Planetary Science Letters, 241, 387–397.

Aharonov, E., Spiegelman, M., and Kelemen, P. (1997) Three-dimensional flow and reaction in porous media: Implications for the Earth's mantle and sedimentary basins. Journal of Geophysical Research: Solid Earth, 102, 14821–14833.

Albaréde, F. (1992) How deep do common basaltic magmas form and differentiate? Journal of Geophysical Research, 97, 10997–11009.

Anderson, A.T. (1974) Evidence for a picritic, volatile-rich magma beneath Mt. Shasta, California. Journal of Petrology, 15, 243–267.

Anderson, A.T., and Wright, T.L. (1972) Phenocrysts and glass inclusions and their bearing on oxidation and mixing of basaltic magmas, Kilauea volcano, Hawaii. American Mineralogist, 57, 188–216.

Bacon, C.R., Bruggman, P.E., Christiansen, R.L., Clynne, M.A., Donnelly-Nolan, J.M., and Hildret, W. (1997) Primitive magmas at five Cascades volcanic fields: Melts from hot, heterogeneous sub-arc mantle. Canadian Mineralogist, 35, 397–424.

Baker, M.B., Grove, T.L., Kinzler, R.J., Donnellynolan, J.M., and Wandless, G.A. (1991) Origin of compositional zonation (high-alumina basalt to basaltic andesite) in the Giant Crater Lava Field, Medicine Lake Volcano, Northern California. Journal of Geophysical Research, 96, 21819–21842.

Baker, M., Grove, T.L., and Price, R. (1994) Primitive basalts and andesites from the Mt. Shasta region, N California—Products of varying melt fraction and water-content. Contributions to Mineralogy and Petrology, 118, 111–129.

Bartels, K.S., Kinzler, R.J., and Grove, T.L. (1991) High pressure phase relations of primitive high-alumina basalts from Medicine Lake volcano, northern California. Contributions to Mineralogy and Petrology, 108, 253–270.

Behn, M.D., and Grove, T.L. (2015) Melting systematics in mid-ocean ridge basalts: Application of a plagioclase-spinel melting model to global variations in major element chemistry and crustal thickness. Journal of Geophysical Research: Solid Earth, 120, 4863–4886.

Blatter, D.L., Sisson, T.W., and Hankins, W.B. (2013) Crystallization of oxidized, moderately hydrous arc basalt at mid- to lower-crustal pressures: Implications for andesite genesis. Contributions to Mineralogy and Petrology, 166, 861–886.

Bloomer, S.H., and Hawkins, J.W. (1987) Petrology and geochemistry of boninite series volcanic-rocks from the Mariana Trench. Contributions to Mineralogy and Petrology, 97, 361–377.

Bouilhol, P., Burg, J.-P., Bodinier, J.-L., Schmidt, M.W., Dawood, H., and Hussain, S. (2009) Magma and fluid percolation in arc to forearc mantle: Evidence from Sapat (Kohistan, Northern Pakistan). Lithos, 107, 17–37.

Bouvier, A.S., Metrich, N., and Deloule, E. (2008) Slab-derived fluids in the magma sources of St. Vincent (Lesser Antilles Arc): Volatile and light element imprints. Journal of Petrology, 49, 1427–1448.

Bowen, N.L., and Schairer, J.F. (1935) The system MgO-FeO-SiO_2. American Journal of Science, 170, 151–217.

Brounce, M.N., Kelley, K.A., and Cottrell, E. (2014) Variations in Fe^{3+}/Fe of Mariana Arc basalts and mantle wedge f_{O_2}. Journal of Petrology, 55, 2513–2536.

Bryant, J.A., Yogodzinski, G.M., and Churikova, T.G. (2010) High-Mg# andesitic lavas of the Shisheisky Complex, Northern Kamchatka: Implications for primitive calc-alkaline magmatism. Contributions to Mineralogy and Petrology, 161, 791–810.

Cagnioncle, A.-M., Parmentier, E.M., and Elkins-Tanton, L.T. (2007) Effect of solid flow above a subducting slab on water distribution and melting at convergent plate boundaries. Journal of Geophysical Research, 112, 1–19.

Cameron, W.E., McCulloch, M.T., and Walker, D.A. (1983) Boninite petrogenesis: chemical and Nd-Sr isotopic constraints. Earth and Planetary Science Letters, 65, 75–89.

Dietrich, V., Emmermann, R., Oberhänsli, R., and Puchelt, H. (1978) Geochemistry of basaltic and gabbroic rocks from the West Mariana Basin and the Mariana Trench. Earth and Planetary Science Letters, 39, 127–144.

Draper, D.S., and Johnston, A.D. (1992) Anhydrous PT phase relations of an Aleutian high-MgO basalt: An investigation of the role of olivine-liquid reaction in the generation of arc high-alumina basalts. Contributions to Mineralogy and Petrology, 112, 501–519.

Elkins-Tanton, L.T., Grove, T.L., and Donnelly-Nolan, J. (2001) Hot, shallow mantle melting under the Cascades volcanic arc. Geology, 29, 631–634.

Falloon, T., and Danyushevsky, L. (2000) Melting of refractory mantle at 1.5, 2 and 2.5 GPa under, anhydrous and H_2O-undersaturated conditions: Implications for the petrogenesis of high-Ca boninites and the influence of subduction components on mantle melting. Journal of Petrology, 41, 257–283.

Ford, C.E., Russell, D.G., Craven, J.A., and Fisk, M.R. (1983) Olivine liquid equilibria - temperature, pressure and composition dependence of the crystal liquid cation partition-coefficients for Mg, Fe^{2+}, Ca and Mn. Journal of Petrology, 24, 256–265.

Frost, D.J., and McCammon, C.A. (2008) The redox state of Earth's mantle. Annual Review of Earth and Planetary Sciences, 36, 389–420.

Gaetani, G.A., and Grove, T.L. (1998) The influence of water on melting of mantle peridotite. Contributions to Mineralogy and Petrology, 131, 323–346.

Gamble, J.A., Smith, I., Graham, I.J., and Kokelaar, B.P. (1990) The petrology, phase relations and tectonic setting of basalts from the Taupo Volcanic Zone, New Zealand and the Kermadec Island Arc-Havre Trough, SW Pacific. Journal of Volcanology and Geothermal Research, 43, 253–270.

Gerya, T.V., Stöckhert, B., and Perchuk, A.L. (2002) Exhumation of high-pressure metamorphic rocks in a subduction channel: A numerical simulation. Tectonics, 21, 6-1–6-19.

Green, D.H. (1973) Experimental melting studies on a model upper mantle composition at high-pressure under water-saturated and water-undersaturated conditions. Earth and Planetary Science Letters, 19, 37–53.

Grove, T.L. (1993) Corrections to expressions for calculating mineral components in "Origin of Calc-Alkaline Series Lavas at Medicine Lake Volcano by Fractionation, Assimilation and Mixing" and "Experimental Petrology of normal MORB near Kane Fracture Zone: 22°–25°N, mid-Atlantic ridge." Contributions to Mineralogy and Petrology, 114, 422–424.

Grove, T.L., and Juster, T.C. (1989) Experimental investigations of low-Ca pyroxene stability and olivine pyroxene liquid equilibria at 1-atm in natural basaltic and andesitic liquids. Contributions to Mineralogy and Petrology, 103, 287–305.

Grove, T.L., Kinzler, R.J., and Bryan, W.B. (1992) Fractionation of mid-ocean ridge basalt (MORB). In Mantle Flow and Melt Generation at Mid-Ocean Ridges, 71, 281–310. American Geophysical Union, Washington, D.C.

Grove, T.L., Parman, S., Bowring, S.A., Price, R., and Baker, M. (2002) The role of an H_2O-rich fluid component in the generation of primitive basaltic andesites and andesites from the Mt. Shasta region, N California. Contributions to Mineralogy and Petrology, 142, 375–396.

Grove, T.L., Elkins-Tanton, L.T., Parman, S., Chatterjee, N., Muentener, O., and Gaetani, G.A. (2003) Fractional crystallization and mantle-melting controls on calc-alkaline differentiation trends. Contributions to Mineralogy and Petrology, 145, 515–533.

Grove, T.L., Chatterjee, N., Parman, S., and Médard, E. (2006) The influence of H_2O on mantle wedge melting. Earth and Planetary Science Letters, 249, 74–89.

Grove, T.L., Till, C.B., and Krawczynski, M.J. (2012) The role of H_2O in subduction zone magmatism. Annual Review of Earth and Planetary Sciences, 40, 413–439.

Grove, T.L., Holbig, E.S., Barr, J.A., Till, C.B., and Krawczynski, M.J. (2013) Melts of garnet lherzolite: experiments, models and comparison to melts of pyroxenite and carbonated lherzolite. Contributions to Mineralogy and Petrology, 166, 887–910.

Hacker, B.R. (2008) H_2O subduction beyond arcs. Geochemistry, Geophysics, Geosystems, 9, 1–24.

Hamada, M., and Fujii, T. (2008) Experimental constraints on the effects of pressure and H_2O on the fractional crystallization of high-Mg island arc basalt. Contributions to Mineralogy and Petrology, 155, 767–790.

Hart, S.R., and Zindler, A. (1986) In search of a bulk-Earth composition. Chemical Geology, 57, 247–267.

Heath, E., Macdonald, R., and Belkin, H. (1998) Magmagenesis at Soufriere Volcano, St. Vincent, Lesser Antilles Arc. Journal of Petrology, 39, 1721–1764.

Helz, R.T., and Thornber, C.R. (1987) Geothermometry of Kilauea Iki lava lake, Hawaii. Bulletin of Volcanology, 49, 651–668.

Hesse, M., and Grove, T.L. (2003) Absarokites from the western Mexican Volcanic Belt: constraints on mantle wedge conditions. Contributions to Mineralogy and Petrology, 146, 10–27.

Hirschmann, M.M. (2000) Mantle solidus: Experimental constraints and the effects of peridotite composition. Geochemistry, Geophysics, Geosystems, 1, 1–26.

Johnson, K.T.M., Dick, H.J.B., and Shimizu, N. (1990) Melting in the oceanic mantle: An ion microprobe study of diopsides in abyssal peridotites. Journal of Geophysical Research, 95, 2661–2678.

Kamenetsky, V.S., Sobolev, A.V., Joron, J.L., and Semet, M.P. (1995) Petrology and geochemistry of cretaceous ultramafic volcanics from Eastern Kamchatka. Journal of Petrology, 36, 637–662.

Katz, R.F., Spiegelman, M., and Langmuir, C.H. (2003) A new parameterization of hydrous mantle melting. Geochemistry, Geophysics, Geosystems, 4, 1–19.

Kawamoto, T., and Holloway, J.R. (1997) Melting temperature and partial melt chemistry of H_2O-saturated mantle peridotite to 11 Gigapascals. Science, 276, 240–243.

Kelemen, P.B., Dick, H.J.B., and Quick, J.E. (1992) Formation of harzburgite by pervasive melt/rock reaction in the upper mantle. Nature, 358, 635–641.

Kelemen, P.B., Whitehead, J.A., Aharonov, E., and Jordahl, K.A. (1995) Experiments on flow focusing in soluble porous media with applications to melt extraction from the mantle. Journal of Geophysical Research, 100, 475–496.

Kelemen, P.B., Hirth, G., Shimizu, N., Spiegelman, M., and Dick, H. (1997) A review of melt migration processes in the adiabatically upwelling mantle beneath oceanic spreading ridges. Philosophical Transactions of the Royal Society A: Mathematical, Physical and Engineering Sciences, 355, 283–318.

Kelemen, P.B., Rilling, J.L., Parmentier, E.M., Mehl, L., and Hacker, B.R. (2003) Thermal structure due to solid-state flow in the mantle wedge beneath arcs. In Inside the Subduction Factory, Geophysical Monograph Series, 138, 293–311. AGU, Washington, D.C.

Kelley, K.A., and Cottrell, E. (2009) Water and the oxidation state of subduction zone magmas. Science, 325, 605–607.

——— (2012) The influence of magmatic differentiation on the oxidation state of Fe in a basaltic magma. Earth and Planetary Science Letters, 329–330, 109–121.

Kelley, K.A., Plank, T., Grove, T.L., Stolper, E.M., Newman, S., and Hauri, E. (2006) Mantle melting as a function of water content beneath back-arc basins. Journal of Geophysical Research, 111, 1–27.

Kelley, K.A., Plank, T., Newman, S., Stolper, E.M., Grove, T.L., Parman, S., and Hauri, E.H. (2010) Mantle melting as a function of water content beneath the Mariana Arc. Journal of Petrology, 51, 1711–1738.

Kent, A., and Elliott, T.R. (2002) Melt inclusions from Marianas arc lavas: Implications for the composition and formation of island arc magmas. Chemical Geology, 183, 263–286.

Kimura, J.-I., and Ariskin, A.A. (2014) Calculation of water-bearing primary basalt and estimation of source mantle conditions beneath arcs: PRIMACALC2 model for WINDOWS. Geochemistry, Geophysics, Geosystems, 15, 1494–1514.

Kimura, J.-I., Hacker, B.R., van Keken, P.E., Kawabata, H., Yoshida, T., and Stern, R.J. (2009) Arc Basalt Simulator version 2, a simulation for slab dehydration and fluid-fluxed mantle melting for arc basalts: Modeling scheme and application. Geochemistry, Geophysics, Geosystems, 10, 1–32.

Kimura, J.-I., Gill, J.B., Kunikiyo, T., Osaka, I., Shimoshioiri, Y., Katakuse, M., Kakubuchi, S., Nagao, T., Furuyama, K., Kamei, A., and others. (2014) Diverse magmatic effects of subducting a hot slab in SW Japan: Results from forward modeling. Geochemistry, Geophysics, Geosystems, 15, 691–739.

Kincaid, C., and Sacks, I. (1997) Thermal and dynamical evolution of the upper mantle in subduction zones. Journal of Geophysical Research, 102, 12295–12315.

Kinzler, R.J. (1997) Melting of mantle peridotite at pressures approaching the spinel to garnet transition: Application to mid-ocean ridge basalt petrogenesis. Journal of Geophysical Research, 102, 853–874.

Kinzler, R.J., and Grove, T.L. (1992a) Primary magmas of midocean ridge basalts 1. Experiments and methods. Journal of Geophysical Research, 97, 6885–6906.

——— (1992b) Primary magmas of midocean ridge basalts 2. Applications. Journal of Geophysical Research, 97, 6907–6926.

——— (1993) Corrections and further discussion of the primary magmas of mid-ocean ridge basalts, 1 and 2. Journal of Geophysical Research, 98, 22339–22347.

Kohut, E.J., Stern, R.J., Kent, A.J.R., Nielsen, R.L., Bloomer, S.H., and Leybourne, M. (2006) Evidence for adiabatic decompression melting in the Southern Mariana Arc from high-Mg lavas and melt inclusions. Contributions to Mineralogy and Petrology, 152, 201–221.

Kushiro, I. (1990) Partial melting of mantle wedge and evolution of island arc crust. Journal of Geophysical Research, 95, 15929–15939.

Kushiro, I., and Sato, H. (1978) Origin of some calc-alkalic andesites in the Japanese Islands. Bulletin Volcanologique, 41, 576–585.

Kushiro, I., Syono, Y., and Akimoto, S. (1968) Melting of a peridotite nodule at high pressures and high water pressures. Journal of Geophysical Research, B, Solid Earth and Planets, 73, 6023–6029.

Langmuir, C.H., Klein, E.M., and Plank, T. (1992) Petrological systematics of mid-ocean ridge basalts: Constraints on melt generation beneath ocean ridges. Mantle Flow and Melt Generation at Mid-Ocean Ridges, 71, 183–280. American Geophysical Union, Washington, D.C.

Lee, C.-T.A., Luffi, P., Plank, T., Dalton, H., and Leeman, W.P. (2009) Constraints on the depths and temperatures of basaltic magma generation on Earth and other terrestrial planets using new thermobarometers for mafic magmas. Earth and Planetary Science Letters, 279, 20–33.

Leeman, W.P., Lewis, J.F., Evarts, R.C., Conrey, R.M., and Streck, M.J. (2005) Petrologic constraints on the thermal structure of the Cascades arc. Journal of Volcanology and Geothermal Research, 140, 67–105.

Leeman, W.P., Schutt, D.L., and Hughes, S.S. (2009) Thermal structure beneath the Snake River Plain: Implications for the Yellowstone hotspot. Journal of Volcanology and Geothermal Research, 188, 57–67.

Li, Y.B., Kimura, J.I., Machida, S., Ishii, T., Ishiwatari, A., Maruyama, S., Qiu, H.N., Ishikawa, T., Kato, Y., Haraguchi, S., and others. (2013) High-Mg adakite and low-Ca boninite from a Bonin Fore-arc Seamount: Implications for the reaction between slab melts and depleted mantle. Journal of Petrology, 54, 1149–1175.

Mitchell, A.L., and Grove, T.L. (2015) Melting the hydrous, subarc mantle: The origin of primitive andesites, Contributions to Mineralogy and Petrology, 170, 1–23.

——— (2016) Experiments on melt–rock reaction in the shallow mantle wedge. Contributions to Mineralogy and Petrology, 171, 1–21.

Miyashiro, A. (1974) Volcanic rock series in island arcs and active continental margins. American Journal of Science, 274, 321–355.

Morishita, T., Dilek, Y., Shallo, M., Tamura, A., and Arai, S. (2011) Insight into the uppermost mantle section of a maturing arc: The Eastern Mirdita ophiolite, Albania. Lithos, 124, 215–226.

Moussallam, Y., Oppenheimer, C., Scaillet, B., Gaillard, F., Kyle, P., Peters, N., Hartley, M., Berlo, K., and Donovan, A. (2014) Tracking the changing oxidation state of Erebus magmas, from mantle to surface, driven by magma ascent and degassing. Earth and Planetary Science Letters, 393, 200–209.

Mullen, E.K., and McCallum, I.S. (2014) Origin of basalts in a hot subduction setting: Petrological and geochemical insights from Mt. Baker, Northern Cascade Arc. Journal of Petrology, 55, 241–281.

Mullen, E.K., and Weis, D. (2015) Evidence for trench-parallel mantle flow in the northern Cascade Arc from basalt geochemistry. Earth and Planetary Science Letters, 414, 100–107.

Mysen, B.O., and Boettcher, A.L. (1975) Melting of a hydrous mantle 1. Phase Relations of natural peridotite at high-pressures and temperatures with controlled activities of water, carbon-dioxide, and hydrogen. Journal of Petrology, 16, 520–548.

Navon, O., and Stolper, E. (1987) Geochemical consequences of melt percolation: the upper mantle as a chromatographic column. The Journal of Geology, 95, 285–307.

Nisbet, E.G. (1984) The continental and oceanic crust and lithosphere in the Archaean: Isostatic, thermal, and tectonic models. Canadian Journal of Earth Sciences, 21, 1426–1441.

Parman, S.W., and Grove, T.L. (2004) Harzburgite melting with and without H_2O: Experimental data and predictive modeling. Journal of Geophysical Research, 109, 1–20.

Parman, S.W., Grove, T.L., Kelley, K.A., and Plank, T. (2011) Along-arc variations in the pre-eruptive H_2O contents of Mariana Arc magmas inferred from fractionation paths. Journal of Petrology, 52, 257–278.

Pearce J.A., and Parkinson I.J. (1993) Trace element models for mantle melting: Application to volcanic arc petrogenesis. In H.M. Prichard, T. Alabaster, N.B.W. Harris, and C.R. Neary, Eds., Magmatic Processes and Plate Tectonics. Geological Society, London, Special Publication, 76, 373–403.

Penniston-Dorland, S.C., Kohn, M.J., and Manning, C.E. (2015) The global range of subduction zone thermal structures from exhumed blueschists and eclogites: Rocks are hotter than models. Earth and Planetary Science Letters, 428, 243–254.

Pichavant, M., and Macdonald, R. (2007) Crystallization of primitive basaltic magmas at crustal pressures and genesis of the calc-alkaline igneous suite: experimental evidence from St Vincent, Lesser Antilles arc. Contributions to Mineralogy and Petrology, 154, 535–558.

Pichavant, M., Mysen, B.O., and Macdonald, R. (2002) Source and H_2O content of high-MgO magmas in island arc settings: An experimental study of a primitive calc-alkaline basalt from St. Vincent, Lesser Antilles. Geochimica et Cosmochimica Acta, 66, 2193–2209.

Pirard, C., and Hermann, J. (2015) Focused fluid transfer through the mantle above subduction zones. Geology, 43, 915–918.

Pirard C., Hermann J., and O'Neill, H.St.C. (2013) Petrology and geochemistry of the crust–mantle boundary in a Nascent Arc, Massif du Sud Ophiolite, New Caledonia, SW Pacific. Journal Petrology 54, 1759–1792.

Poli, S., and Schmidt, M.W. (1995) H_2O transport and release in subduction zones—Experimental constraints on basaltic and andesitic systems. Journal of Geophysical Research, 100, 22299–22314.

——— (2002) Petrology of subducted slabs. Annual Review of Earth and Planetary Science, 30, 207–235.

Portnyagin, M., Hoernle, K., Plechov, P., Mironov, N., and Khubunaya, S. (2007) Constraints on mantle melting and composition and nature of slab components in volcanic arcs from volatiles (H_2O, S, Cl, F) and trace elements in melt inclusions from the Kamchatka Arc. Earth and Planetary Science Letters, 255, 53–69.

Portnyagin, M., Almeev, R., Matveev, S., and Holtz, F. (2008) Experimental evidence for rapid water exchange between melt inclusions in olivine and host magma. Earth and Planetary Science Letters, 272, 541–552.

Putirka, K.D. (2008) Thermometers and barometers for volcanic systems. Reviews in Mineralogy and Geochemistry, 69, 61–120.

Putirka, K. (2016) Rates and styles of planetary cooling on Earth, Moon, Mars, and Vesta, using new models for oxygen fugacity, ferric-ferrous ratios, olivine-liquid Fe-Mg exchange, and mantle potential temperature. American Mineralogist, 101, 819–840.

Putirka, K.D., Perfit, M., Ryerson, F.J., and Jackson, M.G. (2007) Ambient and excess mantle temperatures, olivine thermometry, and active vs. passive upwelling. Chemical Geology, 241, 177–206.

Rowe, M.C., Kent, A.J.R., and Nielsen, R.L. (2009) Subduction influence on oxygen fugacity and trace and volatile elements in basalts across the Cascade Volcanic Arc. Journal of Petrology, 50, 61–91.

Ruscitto, D.M., Wallace, P.J., Johnson, E.R., and Kent, A. (2010) Volatile contents of mafic magmas from cinder cones in the Central Oregon High Cascades: Implications for magma formation and mantle conditions in a hot arc. Earth and Planetary Science Letters, 298, 153–161.

Sisson, T.W., and Bronto, S. (1998) Evidence for pressure-release melting beneath magmatic arcs from basalt at Galunggung, Indonesia. Nature, 391, 883–886.

Sisson, T.W., and Grove, T.L. (1993) Experimental investigations of the role of H_2O in calc-alkaline differentiation and subduction zone magmatism. Contributions to Mineralogy and Petrology, 113, 143–166.

Sobolev, A.V., and Danyushevsky, L.V. (1994) Petrology and geochemistry of boninites from the North Termination of the Tonga Trench: Constraints on the generation conditions of primary high-Ca boninite magmas. Journal of Petrology, 35, 1183–1211.

Sugawara, T. (2000) Empirical relationships between temperature, pressure, and MgO content in olivine and pyroxene saturated liquid. Journal of Geophysical Research: Solid Earth, 105, 8457–8472.

Syracuse, E.M., van Keken, P.E., and Abers, G.A. (2010) The global range of subduction zone thermal models. Physics of the Earth and Planetary Interiors, 183, 73–90.

Takahashi, E., and Kushiro, I. (1983) Melting of a dry peridotite at high pressures and basalt magma genesis. American Mineralogist, 68, 859–879.

Tatsumi, Y. (1981) Melting experiments on a high-magnesian andesite. Earth and Planetary Science Letters, 54, 357–365.

Tatsumi, Y., and Ishizaka, K. (1982) Origin of high-magnesian andesites in the Setouchi volcanic belt, southwest Japan, I. Petrographical and chemical characteristics. Earth and Planetary Science Letters, 60, 293–304.

Tatsumi, Y., and Suzuki, T. (2009) Tholeiitic vs calc-alkalic differentiation and evolution of arc crust: Constraints from melting experiments on a basalt from the Izu-Bonin-Mariana Arc. Journal of Petrology, 50, 1575–1603.

Tatsumi, Y., Sakuyama, M., Fukuyama, H., and Kushiro, I. (1983) Generation of arc basalt magmas and thermal structure of the mantle wedge in subduction zones. Journal of Geophysical Research, 88, 5815–5825.

Till, C.B., Grove, T.L., and Krawczynski, M.J. (2012a) A melting model for variably depleted and enriched lherzolite in the plagioclase and spinel stability fields. Journal of Geophysical Research, 117, 1–23.

Till, C.B., Grove, T., and Withers, A.C. (2012b) The beginnings of hydrous mantle wedge melting. Contributions to Mineralogy and Petrology, 163, 669–688.

Till, C.B., Grove, T.L., Carlson, R.W., Fouch, M.J., Donnelly-Nolan, J.M., Wagner, L.S., and Hart, W.K. (2013) Depths and temperatures of <10.5 Ma mantle melting and the lithosphere-asthenosphere boundary below southern Oregon and northern California. Geochemistry, Geophysics, Geosystems, 15, 864–879.

Tormey, D.R., Grove, T.L., and Bryan, W.B. (1987) Experimental petrology of normal MORB near the Kane Fracture Zone: 22°–25° N, Mid-Atlantic Ridge. Contributions to Mineralogy and Petrology, 96, 121–139.

van Keken, P.E., Kiefer, B., and Peacock, S.M. (2002) High-resolution models of subduction zones: Implications for mineral dehydration reactions and the transport of water into the deep mantle. Geochemistry, Geophysics, Geosystems, 3, 1056, doi:10.1029-2001GC000256.

van Keken, P.E., Hacker, B.R., Syracuse, E.M., and Abers, G.A. (2011) Subduction factory: 4. Depth-dependent flux of H_2O from subducting slabs worldwide. Journal of Geophysical Research, 116, 1–15.

Wada, I., and Behn, M.D. (2015) Focusing of upward fluid migration beneath volcanic arcs: Effect of mineral grain size variation in the mantle wedge. Geochemistry, Geophysics, Geosystems, 16, 3905–3923.

Wade, J.A., Plank, T., Hauri, E.H., Kelley, K.A., Roggensack, K., and Zimmer, M. (2008) Prediction of magmatic water contents via measurement of H_2O in clinopyroxene phenocrysts. Geology, 36, 799.

Wagner, T.P., and Grove, T.L. (1998) Melt/harzburgite reaction in the petrogenesis of tholeiitic magma from Kilauea volcano, Hawaii. Contributions to Mineralogy and Petrology, 131, 1–12.

Waters, L.E., and Lange, R.A. (2015) An updated calibration of the plagioclase-liquid hygrometer-thermometer applicable to basalts through rhyolites. American Mineralogist, 100, 2172–2184.

Watt, S.F.L., Pyle, D.M., Mather, T.A., and Naranjo, J.A. (2013) Arc magma compositions controlled by linked thermal and chemical gradients above the subducting slab. Geophysical Research Letters, 40, 2550–2556.

Weaver, S.L., Wallace, P.J., and Johnston, A.D. (2011) A comparative study of continental vs. intraoceanic arc mantle melting: Experimentally determined phase relations of hydrous primitive melts. Earth and Planetary Science Letters, 308, 97–106.

Weber, R.M., Wallace, P.J., and Dana Johnston, A. (2011) Experimental insights into the formation of high-Mg basaltic andesites in the trans-Mexican volcanic belt. Contributions to Mineralogy and Petrology, 163, 825–840.

Wilson, C.R., Spiegelman, M., van Keken, P.E., and Hacker, B.R. (2014) Fluid flow in subduction zones: The role of solid rheology and compaction pressure. Earth and Planetary Science Letters, 401, 261–274.

Yang, H.J., Kinzler, R.J., and Grove, T.L. (1996) Experiments and models of anhydrous, basaltic olivine-plagioclase-augite saturated melts from 0.001 to 10 kbar. Contributions to Mineralogy and Petrology, 124, 1–18.

Yoder, H.S., and Tilley, C.E. (1962) Origin of basalt magmas—An experimental study of natural and synthetic rock systems. Journal of Petrology, 3, 342–532.

Manuscript received March 24, 2016
Manuscript accepted December 16, 2016
Manuscript handled by Keith Putirka